



JIMMA UNIVERSITY
JIMMA INSTITUTE OF TECHNOLOGY
FACULTY OF ELECTRICAL AND COMPUTER ENGINEERING
GRADUTE PROGRAM IN ELECTRICAL POWER ENGINEERING

**DESIGN AND SIMULATION OF HYBRID OFF-GRID BIOMASS-SOLAR PV POWER
GENERATING SYSTEM CASE STUDY ON JIMMA ZONE, GUMMAY WEREDA**

BY
BIRHANU BELETE

A thesis submitted to faculty of electrical and computer engineering, Jimma institute of technology in partial fulfillment of the requirements for the degree of masters of Science in electrical power engineering

Advisor: Mr. Molla Biweta (Asst. Prof)

Co-advisor: Mr. Abraham Alem (M.Sc.)

November, 2017

Jimma-Ethiopia

JIMMA UNIVERSITY
JIMMA INSTITUTE OF TECHNOLOGY
FACULTY OF ELECTRICAL AND COMPUTER ENGINEERING
GRADUTE PROGRAM IN ELECTRICAL POWER ENGINEERING

DESIGN AND SIMULATION OF HYBRID OFF-GRID BIOMASS-SOLAR PV POWER
GENERATING SYSTEM CASE STUDY ON JIMMA ZONE , GUMMAY WEREDA

by

BIRHANU BELETE

APPROVED BY BOARD OF EXAMINERS

Abera Jote (Asst. Prof)

*Chairman, Faculty of Electrical
and Computer engineering*

Signature

Date

Getachew Bekele (Ass. Prof)

External Examiner

Signature

Date

Tefera Mekonnen (Asst. Prof)

Internal Examiner

Signature

Date

Acknowledgement

Firstly and most importantly I would like to thank the almighty God, who gave me time, health and wisdom. Without him at my side I would not have been able to complete this thesis. A special thanks to my advisor, Mr.Molla Biweta(Asst.prof.) and my co-advisor Mr. Abreham Alem(MSc.) for their valuable guidance, support and motivation during my thesis work. Second my special thanks goes to Dr. Kinde Anley(Asst.Prof), Mr.Melaku Mathe-wos(MSc.),Mr.Mengistu Fentaw(MSc.) for their valuable comments and suggestions. Third I owe my greatest gratitude to my parents especially to my beloved wife and daughter, who have been the inspirations of my life; your passion for Love has contributed immensely to the completion of this study; this is for you. I am grateful to the Faculty of Electrical Engineer-ing at the Jimma Institute of Technology for providing me the excellent work environment during my study. Let my acknowledgment extend to my classmates, friends, instructors and colleagues in and outside the University. I would like to appreciate all for their friendship and support during my stay at Jimma University. Finally, I acknowledge all other who have helped me and whose names could not be accommodated in this brief acknowledgment.

Many thanks for all who wished my success!!!

Declaration

I, the undersigned, declare that this MSc thesis is my original work, has not been presented for fulfillment of a degree or professional qualification in this or any other university, and all sources and materials used for the thesis have been acknowledged.

Birhanu Belete

Researcher Name

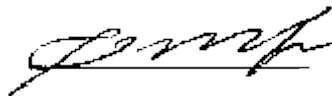
Signature

Date

The thesis entitled, design and Simulation of hybrid Biomass-solar PV power generating case study Jimma Zone, Gumay Woreda submitted by Birhanu Belete to Jimma University in partial fulfillments for the degree of MSc. in Electrical Power Engineering is here by recommended for final evaluation and examination.

Molla Biweta (Asst. Prof)

Major Advisor Name


Signature

15/12/2017
Date

Abraham Alem (MSc.)

Co-Advisor Name

Signature

Date

CONTENTS

Acknowledgment	i
Declaration	ii
Table of contents	iii
List of Figures	v
List of Tables	vi
Acronyms	vii
Abstract	viii
Chapter 1: Introduction	1
1.1 Back ground	1
1.2 Problem Statement	2
1.3 Motivation	2
1.4 Objective	2
1.4.1 General objective	2
1.4.2 Specific objective	2
1.5 Limitation of the study	3
1.6 Structure of the Thesis	3
Chapter 2: Theoretical Background	4
2.1 Literature review	4
2.2 Basic theories of renewable Energy	6
2.2.1 Basic theories of solar Energy	6
2.2.2 Basic theories of Biomass Energy	11
2.3 Syngas in Internal Combustion Engine	16
2.4 Storage Battery	17
2.5 Hybrid Power System	18
2.6 Fuzzy Logic Control	21
2.6.1 Introduction to fuzzy logic	21
2.6.2 Membership Function	22
2.6.3 Linguistic Variable	23
Chapter 3: Potential Resource assessment and Load Estimation	25
3.1 Overview of the selected site	25
3.2 Solar Energy potential assessment	25
3.2.1 Solar insolation data and estimation	26
3.2.2 Data Comparison of Global solar radiation of NMA and NASA	30

3.3	Bio-mass Energy resource	31
3.4	Load Estimation	32
Chapter 4: Modeling,Simulation and Cost Estimation of hybrid power system		37
4.1	Proposed Hybrid system	37
4.2	Modeling and Designing of PV system	37
4.2.1	PV system Designing and Sizing	37
4.2.2	Equivalent circuit and Mathematical modeling of PV system	39
4.3	MATLAB Modeling of PV system	41
4.3.1	Effect of Solar radiation variation on PV model	41
4.3.2	Effect of Temperature variation on PV model	42
4.3.3	Simulation result of PV array	43
4.3.4	DC-DC converter	45
4.3.5	Design and modeling of three phase inverter	48
4.3.6	Storage Battery Designing and sizing	48
4.4	Modeling and Design of Biomass system	50
4.4.1	Biomass Gasification parameters	50
4.4.2	Gasifier Height	52
4.4.3	Gas Production rate	52
4.4.4	Biomass system Designing and sizing	52
4.5	Modeling of Fuzzy controller for the hybrid system	53
4.5.1	Fuzzy controller design	53
4.6	Modeling of Fuzzy Logic control rules	57
4.7	Overall Fuzzy Logic Control System	58
4.8	Matlab Simulation Result of Fuzzy Logic Control	59
4.9	Cost Estimation of the system	60
4.9.1	Cost Evaluation of Solar PV Power Generation	60
4.9.2	Investment Cost PV and Battery	60
4.9.3	Life cycle cost(LCC) of PV system	60
4.9.4	Investment Cost of Biomass Gasifier and Dual Fuel Generator	61
Chapter 5: Conclusion and Recommendation		64
5.1	Conclusion	64
5.2	Recommendation	65
Bibliography		66

Appendix A:Matlab Program	70
Annex A:Data sheet of solar panel	74
Annex B:Data sheet of Battery	77

LIST OF FIGURES

Figure 2.1	p-n junction in a simple circuit [18]	8
Figure 2.2	PV cell formed by n- and p-layers [18]	8
Figure 2.3	PV cell cennection [21]	9
Figure 2.4	Monocrystalline, polycrystalline, and amorphous solids [18]	10
Figure 2.5	Gassification process [25]	12
Figure 2.6	Biomass Power plant [23]	15
Figure 2.7	DC coupled Configuration [32]	19
Figure 2.8	AC coupled Configuration [32]	20
Figure 2.9	Hybrid coupled Configuration [32]	21
Figure 2.10	Classical sets [33]	21
Figure 2.11	Fuzzy sets [34]	22
Figure 2.12	Membership Function [35]	22
Figure 3.1	Map of Gumay,Jimma, Ethiopia [source:Google map]	25
Figure 3.2	Average Monthly sunshine hour [Source: NMA, Jimma branch] . . .	26
Figure 3.3	Solar Radiation of Gumay woreda[source:Author of thesis]	30
Figure 3.4	Data Comparison of NMA and NASA [source:Author of thesis] . . .	30
Figure 3.5	Average Yearly coffee seed production [source:Author of thesis] . . .	32
Figure 3.6	Daily Load Curve of Pera [source:Author of thesis]	36
Figure 4.1	proposed Hybrid system[source:Author of thesis]	37
Figure 4.2	Equivalent circuit of single solar cell [41]	39
Figure 4.3	PV array MATLAB model[source:Author of thesis]	41
Figure 4.4	I-V curve for different solar radiation [source:Author of thesis]	42
Figure 4.5	P-V curve for different solar radiation [source:Author of thesis]	42
Figure 4.6	I-V curve for different cell Temperature [source:Author of thesis] . . .	43
Figure 4.7	P-V curve for different cell Temperature [source:Author of thesis] . .	43
Figure 4.8	input radiation data [source:Author of thesis]	44
Figure 4.9	input temperature data [source:Author of thesis]	44
Figure 4.10	Matlab simulation Result of PV voltage [source:Author of thesis] . . .	44
Figure 4.11	Equivalent circuit of DC-DC Boost converter [48]	46
Figure 4.12	Mode 1- Equivalent circuit of boost converter during ton [49]	46
Figure 4.13	Mode 2- Equivalent circuit of boost converter during toff [49]	46

Figure 4.14 Simulated response of output voltage of Boost converter [source:Author of thesis]	47
Figure 4.15 SPWM System Model [49]	48
Figure 4.16 Battery Model [source:Author of thesis]	50
Figure 4.17 Block Diagram of fuzzy logic controller[source:Author of thesis] . . .	54
Figure 4.18 Fuzzy control model[source:Author of thesis]	55
Figure 4.19 Membership function for Solar Power[source:Author of thesis]	55
Figure 4.20 Membership function for Biomass Power[source:Author of thesis] . . .	56
Figure 4.21 Membership function for Battery Power[source:Author of thesis] . . .	57
Figure 4.22 Membership function for output Power[source:Author of thesis]	57
Figure 4.23 Fuzzy Logic Rules[source:Author of thesis]	58
Figure 4.24 Overall Fuzzy logic Control System[source:Author of thesis]	59
Figure 4.25 Simulation result when all energy forms are available[source:Author of thesis]	59

LIST OF TABLES

Table 3.1	Monthly average of daily sunshine hour for Gumay[Source:NMA Jimma Branch	26
Table 3.2	Solar Hour angle of a day	28
Table 3.3	Monthly solar radiation at the study site	29
Table 3.4	Data Comparison	30
Table 3.5	Average yearly coffee Production	31
Table 3.6	Energy Consumption of Household	33
Table 3.7	Energy Consumption of primay school and health center	35
Table 4.1	Electrical specification for KC200GT panel	38
Table 4.2	Linguistic variable and parameter range for the solar power input . . .	56
Table 4.3	Linguistic variable and parameter range for the Biomass power input .	56
Table 4.4	Linguistic variable and parameter range for the battery power input .	57
Table 4.5	The used cost data	60
Table 4.6	System cost of PV with its accessory	61
Table 4.7	Biomass Gasification investment cost Breakdown	62
Table 4.8	Economic Parameter for the Biomass Power Plant [57]	62

Acronyms

HES	Hybrid Energy System
MATLAB	Matrix Laboratory
NASA	National Aeronautics and Space Administration
NMA	National Meteorology Agency
HOMER	Hybrid Optimization Model For Electric Renewable
IC	Internal Combustion
MGV	Main gas valve
AH	Amper Hour
MOM	Mean of max
COA	Center of area
SSH	Sunshine hour
PWM	Pulse width Modulation
CCM	Continuous conduction mode
LHV	Lower heating value

Abstract

Ethiopia is in Rapid Economic growth and the growth of the country depends on both urban and rural areas growth. On the other hand the demand of Electric energy grow rapidly with Economic growth. Today only 27.2% of the population have access to electricity and this becomes a challenge for the further growth of the county especially for rural areas. An off-grid hybrid energy system have been attracting to supply electricity to rural areas in all aspects like, reliability, sustainability and environmental protections, especially for communities living far in areas where grid extension is not appropriate.

The purpose of this thesis is to Design and simulate an off-Grid Fuzzy Logic Controller Based Hybrid Biomass-Solar PV power generating system to electrify 200 households in pera Village, Gumay woreda which is located 75 kilo meter west of Jimma, Ethiopia. The study area has an average sunshine hour data of 7.05 hours per day and by using Angestron model the sunshine hour data has converted to radiation data. Hence, the study area has an average solar radiation of 5.38kwh/day. A ten year average of 1845 metric ton coffee husk biomass resource has dumped without any economic advantage and it becomes a national waste. Since the biomass resource becomes a national waste this study hybridized biomass with solar PV as a primary source to supply electricity directly to the load and to charge battery bank when excess generation is happened. The community's load has been suggested for lighting, water pumping, school and health clinic equipment load, television, radio, communal loads and industrial loads. Accordingly, A load demand of 245.16kwh/day with a peak load of 38.85kw was involved in the design and simulation of the power system.

In order to supply the load demand of the study area the contribution of biomass to solar PV was 82.6% to 17.4%. The reason behind this contribution is the fact that biomass becomes a waste for the community and this study needs to avoid its adverse environmental effect by designing a biomass plant that utilizes 70% of the biomass resource.

Fuzzy logic controller has been used to decide the output power depending on the available resource. To do this, the hybrid system was modeled on matlab/simulink and fuzzy rule have been written on fuzzy logic rule editor. Then the rules has been loaded to the fuzzy logic controller and simulation have been performed. On the simulation result, it is observed that the fuzzy logic controller was able to control the available resource and supply to the load.

Finally, cost estimation has been performed using analytical method. Accordingly the total life cycle cost of the system becomes \$134,817.962.

Key Words : Solar PV, MATLAB, Biomass, Fuzzy Logic Control, Hybrid

CHAPTER 1

INTRODUCTION

1.1 Back ground

Energy plays a crucial role in technological and economic development of present society. It has always been the key to humans greatest dream of a better world. But now many villages in the world live in isolated areas far from the main utility grid [1]. Access to modern energy, especially in rural, remote areas would help significantly to reduce poverty, to get better health care and education, to facilitate modern communication and information systems. Further, it will reduce city migration and deforestation as well as pollutant gas emission to the environment. The development of renewable energy based on locally available resource should play a key role in this regard.

Renewable resources are abundant. As a single renewable energy source such as PV, wind or biomass is not 100 % reliable due to unavailability of sunshine in night hours or in rainy reason, variation of wind speed and uncertainty in availability of biomass, it is advisable to use a combination of two or more energy sources for reliable and uninterrupted power supply. Many commercial technologies are available to connect these resources, and their costs can be minimized through proper equipment sizing and load matching. When More than two energy systems form a hybrid energy system (HES), usually, they require power conditioning equipment such as a controller and an energy storage system. Hybrid Energy system, which has a longer life cycle, is the best option where grid connectivity is practically impossible or uneconomical. Hybrid renewable system is a viable alternative solution as compared to systems which rely entirely on Traditional biomass. Diesel generator may not be cost-effective for supply of energy due to high cost of fuel as well as fuel transportation cost to remote areas. Moreover, Diesel generator sets discharge large quantity of carbon dioxide and other harmful pollutants to the atmosphere and cause a serious threat to the environment. This led planners and researchers to find an alternative environmental friendly and sustainable solution for supplying power to remote off-grid areas [2].

Ethiopia is one of the non-oil producing and developing countries with a population 107,534,882 in 2018 [3]. Out of which 79.8% [3]of the population live in rural areas and according to the total access to electricity in the country is about 27.2% [4]. The demand of electrical energy grow rapidly with an economic growth. For an economic growth rate of 7-10% the resulting electrical energy demand growth is about 17%. But Ethiopia is developing at an economic growth rate of 8-12% indicates that the electrical energy demand growth is more

than 17%. [5].

1.2 Problem Statement

Energy and water are the key to modern life and provides the basic necessity for sustained economic development. Unfortunately, not everybody has the fortune of enjoying all the benefits from these two things. About 72.8% [4] of the population in Ethiopia lacks access to electricity and therefore to a large number of electricity based services and commodities. About 90% of the rural population rely on firewood for cooking, 70% on Kerosene lamps to light their home at night [6]. Modern means of entertainment are either not known to them or are a distance possibility. Many peoples die every year from drinking polluted water, while others suffer from the lack of basic medical services. Illiteracy denies many people any possibility of gaining access to better opportunities. Firewood is still the main source of fuel in most rural communities despite the alarming deforestation, dangerous to health and the amount of work needed to collect. Survival remains the name of the game for many people in remote rural areas. The reason for this is the lack of access to reliable and affordable energy source.

1.3 Motivation

People living in rural part of Ethiopia are using Kerosene lamp or candles to lit their home at night. In the study area students use these light options for self learning or to do their homework at night. Since kerosene lamps release particulate matters that are dangerous to health it adversely affects the health of the students. On the other hand the study area has very high renewable energy resource.

Therefore, the very good potential of solar and biomass resource at the selected site have motivated me to design and simulate a system that can electrify the area by stand-alone hybrid PV-Biomass system.

1.4 Objective

This thesis work has the following general and specific objectives

1.4.1 General objective

The main objective of this study is to Design and Simulate hybrid biomass-solar energy system using matlab/simulink software.

1.4.2 Specific objective

The specific objective of this thesis are:

- * To assess the energy consumption of the community around the site.
- * To assess the potential of biomass and solar energy source around Gumay woreda.
- * To design and simulate biomass-solar hybrid power system on MATLAB/SIMULINK software
- * To design the Fuzzy logic controller for the system
- * To draw a recommendation for further implementation of optimized hybrid power supply system for the site under consideration

1.5 Limitation of the study

This thesis is intended to design a hybrid power system with Fuzzy logic controller for the village in Gumay woreda. From the available different configurations of the hybrid system, this thesis has focused on solar/Biomass/Battery system. In this thesis the battery bank is used as a backup during night time and decreased renewable energy potential. MATLAB software is used for modeling of the system. The daily solar radiation and the Biomass resource are collected from office of National Meteorology Agency (NMA) Jimma branch and Gumay woreda coffee quality office respectively. The study will also include design, modeling and simulation of fuzzy logic control system.

The scope of the thesis is to supply electric power to 200 household, one primary school and one health center.

1.6 Structure of the Thesis

This thesis is organized into six chapters. The first chapter introduces about the background, problem statement, motivation, objective, scope and significant of the study and limitation of the study.

Chapter two discusses the theoretical overviews of solar energy (PV system), Biomass energy, Hybrid system of Renewable energy and fuzzy logic controller. Chapter three gives the Potential assessments of renewable energies around Gumay woreda. The assessment is based on the data obtained from both Local Source (from National Meteorology Agency) and International source (from NASA). Hybrid system designing and modeling are presented in chapter four. Chapter five presents the cost estimation of the system. In chapter Six, conclusions are drawn concerning to the simulation result and recommendation also produced as response to conclusions.

CHAPTER 2

THEORETICAL BACKGROUND

2.1 Literature review

M. Chegaar et al, 1998 [7] described how an empirical model, originally formulated by Sivkov to compute the monthly global irradiation, has been modified to make it fit for some Algerian and Spanish sites. Appropriate parameters have been introduced. The monthly average daily values of global irradiation incident on a horizontal surface at some Algerian and Spanish meteorological stations are computed by this method using sunshine hours and minimum air-mass. The obtained values, for Algeria, are then compared to those calculated by M. Capderou. Measurements of global solar irradiation on horizontal surface at some Spanish meteorological stations, published by J Canada, are compared to predictions made by this model. The agreement between the measured and computed values and those estimated by this model is remarkable as they say. Getachew Bekele, 2009 [8] investigated the way of supplying electric energy from solarwind hybrid resources to remotely located communities detached from the main grid line in Ethiopia. He used sunshine hour data collected over a period of more than 10 years at four geographically different locations (Addis Ababa, Mekele, Nazret, and Debrezeit). Based on the sunshine duration data, the monthly average daily sunshine amount for each of the places has been computed. The estimation of monthly average solar radiation was done with the help of an empirical equation by Duffie and Beckman, 1991 and using regression coefficients specific to the sites in question. The results indicated an abundance of solar energy potential. Siddhartha Gobina, 2012 [9], designs stand alone solar, wind and Biomass hybrid power system to meet the load demand of the village at Sagar Island using genetic algorithm. The decision variables he considered for this optimization processes are numbers of pv-panels, numbers of wind turbines and capacity of biomass generator. The monthly average solar radiation and wind speed of the study area are converted in to hourly solar irradiance and hub height speed; here minimum values are considered for optimization process. This writer also tries to compares per unit energy cost and co2 emission emission of Biomass generator and diesel generator. Finally research results indicates hybrid power system considering Biomass has minimum per unit energy cost and less co 2 emission as compared to diesel generator consisting hybrid power system. Biomass is economically feasible but in this paper the Biomass is wood so still it facilitates deforestation. Ramos-Hernanz et.al., 2012 [10] have compared the five and eight parameter PV Simulation Models in time domain by using matlab/simulink, to achieve an I-V curve

similar to the manufacturer's data sheet. However, these models have been developed with a large number of assumptions. Since he has considered a large number of assumption in order for curve fitting he can't determine the real performance of the PV system .

Bikaneria et.al, 2013 [11] have studied in this paper one diode photovoltaic cell model are focused. Simulation studies are carried out with different temperature. But he haven't seen the impact of irradiance variation on the PV performance.

Venkateswarlu and Raju, 2013 [12] the study of photovoltaic systems in an efficient manner requires a precise knowledge of the IV and PV characteristic curves of photovoltaic modules. A Simulation model for simulation of a single solar cell and two solar cells in series has been developed using sim electronics (matlab/simulink) environment and is presented. A solar cell block is available in sim electronics, which was used with many other blocks to plot I-V and P-V characteristics under variations of parameters considering one parameter variation at a time. Effect of two environmental parameters of temperature and irradiance variations could also be observed from simulated characteristics.

Bonkougou et al., 2013 [13] this paper presents a photovoltaic (PV) cell to module simulation model using the single-diode five parameter models. The model was implemented in matlab software and the results have been compared with the data sheet values and characteristics of the PV module in Standard Test Conditions (STC). Parameters values were extracted using Newton Raphsons method from experimental Current (I)-Voltage (V) characteristics of Solar ex MSX60 module. The results obtained are in good agreement with the experimental data provided by manufacturer. The approach can thus, be very useful for researchers or engineers to quickly and easily determine the performance of any photovoltaic module. Madhu Prabhuraj et al., 2013 [14], have assessed the locally available resources such as sun light, wind, water and biogas for efficient and reliable power generation in Tamilnadu, India. Here fuzzy logic controller is used to control the power plant which will generate power. The controller does the analyses of the change in load and accordingly changes the mode of operation of the system. When the solar and wind modes are not sufficient, the biogas power generator is switched on and synchronized with the available grid to meet the demand. Generally it is possible to say in one way or the other the above hybrid power generating system includes 1) Wood as a source of power in which most of the biomass plants is exercising. This brings drought because of deforestation and finally global warming. 2) Diesel generator as alternative source of power. But the cost of fuel is increasing day by day and environment pollution is high. The proposed hybrid Solar pv/micro-hydro and Biomass power generating system avoids the above discussed issues. There is no battery

because Biomass is standby backup source for the system. The Biomass input is by product of coffee (coffee husk) which can be easily accessible.

Akikur et al., 2013 [15] reviewed many hybrid systems published by researchers for off-grid rural electrification. The review of the last 12 years of research, demonstration and case studies revealed that solar energy can be a viable solution for provision of power throughout the world, especially electrification of rural off-grid locations in eco-friendly and cost-effective manner. Both the stand-alone solar PV system and the hybrid solar PV system will provide excellent electrification solution for any load in rural locations far away from the grid.

Ahmad et al., 2010 [16] studied the economic and environmental aspects of different renewable energy sources for rural electrification in Iran by using HOMER. The simulation results indicated that a hybrid power system comprising 150 kW photovoltaic system together with 100 kW wind generator system, 25 kW fuel cell and battery storage of 6 h of autonomy (equivalent to 6 h of average load) would be a feasible solution for distributed generation of electric power for stand-alone applications at remote locations.

2.2 Basic theories of renewable Energy

The energy which is harvested from the natural resources like sunlight, wind, tides, geothermal heat etc. is called Renewable Energy. Renewable energy sources also called non-conventional type of energy are the sources which are continuously replenished by natural processes. Such as, solar energy, biomass energy, wind energy and hydro power etc., are some of the examples of renewable energy sources. A renewable energy system convert the energy found in sunlight, falling-water, wind, sea-waves, geothermal heat, or biomass into a form, which we can use in the form of heat or electricity. The majority of the renewable energy comes either directly or indirectly from sun and wind and can never be fatigued, and therefore they are called renewable. As these resources can be naturally replenished, for all practical purposes, these can be considered to be limitless unlike the tapering conventional fossil fuels. The global energy crunch has provided a renewed impulsion to the growth and development of Clean and Renewable Energy sources.

2.2.1 Basic theories of solar Energy

The sun is free, silent, and nonpolluting source of energy and is responsible for all lifeforms on the planet. Its use for energy generation can be direct or indirect. Indirect solar energy is related primarily to wind power, hydropower, photosynthesis, sea tidal energy. The sun does not reach directly only one point on Earth during each day. Also, its intensity does not stay unchanged when available, and a utilization factor is fundamental in the definition

of how economically feasible it may be to harness the sun's energy [17]. Solar energy is the energy force that sustains life on Earth for all plants, animals, and people. It provides a compelling solution for all societies to meet their needs for clean, abundant sources of energy in the future. The source of solar energy is the nuclear interactions at the core of the Sun, where the energy comes from the conversion of hydrogen into helium. Sunlight is readily available, secure from geopolitical tensions, and poses no threat to our environment and our global climate systems from pollution emissions.

Solar energy is primarily transmitted to the Earth by electromagnetic waves, which can also be represented by particles (photons). The Earth is essentially a huge solar energy collector receiving large quantities of solar energy that manifest in various forms, such as direct sunlight used for plant photosynthesis, heated air masses causing wind, and evaporation of the oceans resulting as rain, which forms rivers and provides hydro power [18].

Solar energy can be tapped directly (e.g., PV); indirectly as with wind, biomass, and hydro power; or as fossil biomass fuels such as coal, natural gas, and oil. Sunlight is by far the largest carbon-free energy source on the planet. PV cells are used to generate electrical energy by converting solar radiation into direct current electricity using semiconductors that exhibit the photovoltaic effect. Photovoltaic power generation employs solar panels composed of a number of solar cells containing a photovoltaic material. Materials presently used for photovoltaics include monocrystalline silicon, polycrystalline silicon, amorphous silicon, cadmium telluride, and copper indium gallium selenide/sulfide. Due to the growing demand for renewable energy sources, the manufacturing of solar cells and photovoltaic arrays has advanced considerably in recent years [19]. **A.Operation of Solar PV cells :-** Electricity can be produced from sunlight through a process called the photo voltaic (PV) effect, where "photo" refers to light and "voltaic" to voltage. The term describes a process that produces direct electrical current from the radiant energy of the Sun. The PV effect can take place in solid, liquid, or gaseous material; however, it is in solids, especially semiconductor materials, that acceptable conversion efficiency have been found. Solar cells are made from a variety of semiconductor materials and coated with special additives. The most widely used material for the various types of fabrication is crystalline silicon, representing over 90% of global commercial PV module production in its various forms.

A typical silicon cell, with a diameter of 10 cm., can produce more than 1 W of direct current (DC) electrical power in full sun. Individual solar cells can be connected in series and parallel to obtain desired voltages and currents. These groups of cells are packaged into standard modules that protect the cells from the environment while providing useful voltages and

currents. PV modules are extremely reliable because they are solid state and have no moving parts. PV devices or solar cells are made from semiconductor materials. Semiconductor materials are those elements or compounds that have conductivity intermediate to that of metals or insulators.

The most common solar cells are basically large pn (thought of as positivenegative) junction diodes that use light energy (photons) to produce DC electricity. No voltage is applied across the junction; rather, a current is produced in the connected load when the cells are illuminated. A diode is an electronic device that permits unidirectional current. The solar cell is fabricated by having n- and p-layers, which make up a junction (Figure 2.1 and Figure 2.2). The pn junction is formed by combining doped semiconductor materials such as Si or GaAs [18].

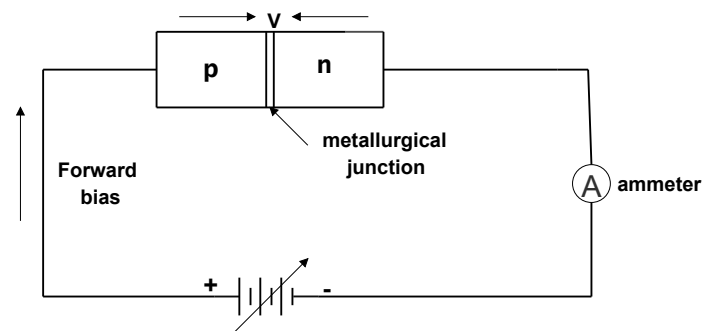


Figure 2.1: p-n junction in a simple circuit [18]

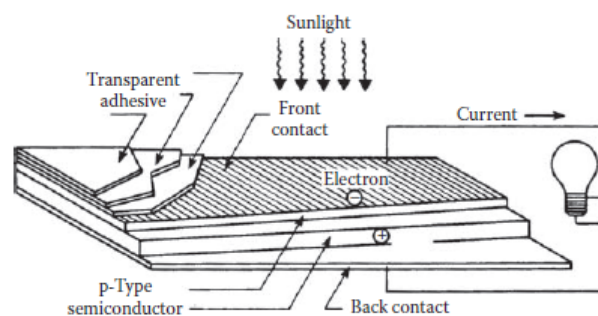


Figure 2.2: PV cell formed by n- and p-layers [18]

The amount of current generated by a PV cell depends on its efficiency (type of PV cell), its size (surface area) and the intensity of sunlight striking the surface. The electrical output from a single cell is small, so multiple cells are connected and encapsulated (usually glass covered) to form a module (also called a panel). Cells can be connected either in series or in parallel [20].

B.Series and parallel connection of PV cell :- Higher power, using low power solar PV cells, can be obtained by making series and parallel connection of cells. Series connection is done in order to increase the output voltage, while parallel connection is done in order to increase the current output. While making parallel and series connection of PV cell it is assumed that all cells have the same characteristic. i.e. They are identical in all aspects [21].when two cells, which are identical, are connected in series, the output voltage of the two cells added while the current through the combination will be the same as that of the single cell as shown in the figure.

When two cells are connected in parallel the current from the two cells will be added while, the voltage of the combination will remain the same as that of a single cell as shown in figure.

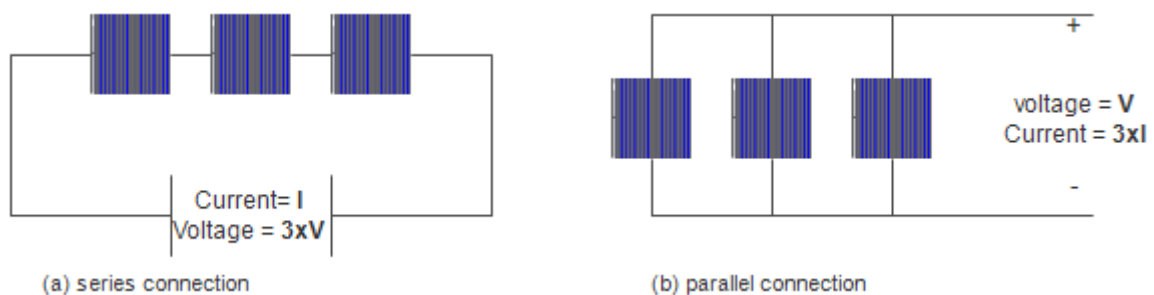


Figure 2.3: PV cell connection [21]

C.Type and Purity of Material :- Solar cells for terrestrial applications are typically made from silicon as single-crystal, poly-crystalline, or amorphous solids. Single-crystal silicon is the most efficient because the crystal is free of grain boundaries, which are defects in the crystal structure caused by variations in the lattice that tend to decrease the electrical and thermal conductivity of the material. They can be thought of as barriers to electron flow. Poly-crystalline silicon has obvious grain boundaries; the portions of single crystals are visible to the naked eye. Amorphous silicon (a-Si) is the non-crystalline form of silicon where the atoms are arranged in a relatively haphazard way. Due to the disordered nature of the material, some atoms have a dangling bond that disrupts the flow of electrons. A dangling bond occurs when an atom is missing a neighbor to which it would be able to bind. Amorphous silicon has lowest power conversion efficiency of the three types, but is the least expensive to produce. Figure 2.4 depicts these types of solids pictorially.

Mono-crystalline silicon. Cells are made from an ingot of a single crystal of silicon, grown in high-tech labs, sliced, then doped and etched. For commercial terrestrial modules, efficiency typically range from about 15-20%. Modules made of this type of cell are the most mature

on the market. Reliable manufacturers of this type of PV module offer guarantees of up to 20-25 years at 80% of nameplate rating.

Polycrystalline silicon:-These cells are made up of various silicon crystals formed from an ingot. They are also sliced and then doped and etched. They demonstrate conversion efficiency slightly lower than those of monocrystalline cells, generally from 13 to 15%. Reliable manufacturers typically guarantee polycrystalline PV modules for 20 years. **Amorphous silicon.** The term amorphous refers to the lack of any geometric cell structure. Amorphous modules do not have the ordered pattern characteristic of crystals as in the case of crystalline silicon. Commercial modules typically have conversion efficiency from 5 to 10%. Most product guarantees are for 10 years, depending on the manufacturer. The technology has yet to gain widespread acceptance for larger power applications largely due to shorter lifetimes from accelerated cell degradation in sunlight (degradation to 80% of original output in most cases). However, amorphous PV has found wide appeal for use in consumer devices (e.g., watches and calculators).

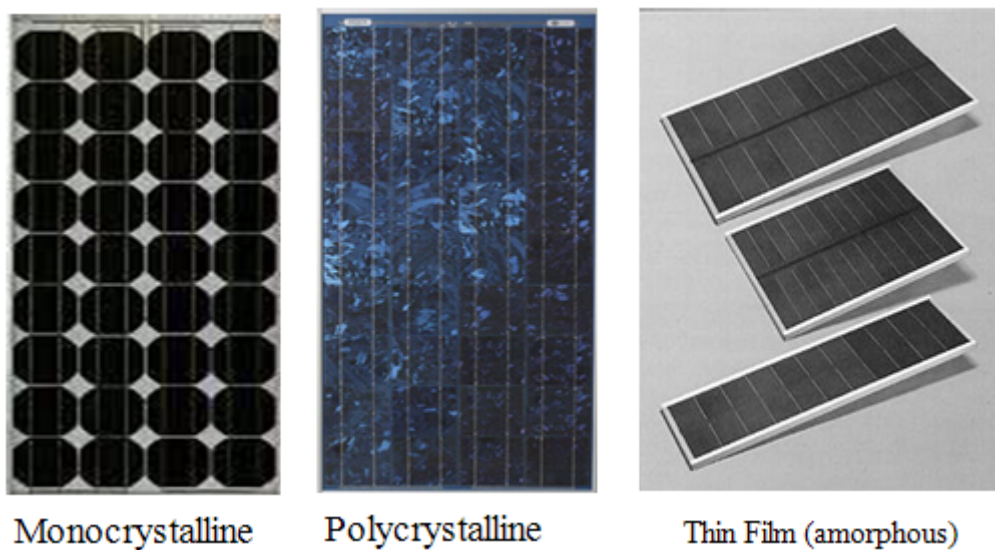


Figure 2.4: Monocrystalline, polycrystalline, and amorphous solids [18]

It does have the advantage for some grid-tied or water-pumping systems in that higher voltage modules can be produced more cheaply than their crystalline counterparts. Another limiting factor to efficiency is that of traps in the material. Traps are semiconductor material impurities in the depletion region and can greatly increase recombination of electrons and holes. Recombination reduces V_{oc} , in turn reducing the fill factor and efficiency.

2.2.2 Basic theories of Biomass Energy

Biomass is a scientific term for living matter, more specifically any organic matter that has been derived from plants as a result of the photosynthetic conversion process. The word biomass is also used to denote the products derived from living organisms wood from trees, harvested grasses, plant parts, and residues such as stems and leaves, as well as aquatic plants. Biomass is renewable source of energy produced in nature through photosynthesis achieved by solar energy conversion and it play dual role in greenhouse gas mitigation [22].

A. Gasification process of Biomass Energy :- Biomass gasification is the conversion of solid or liquid feedstock in to useful and convenient gaseous fuel that can be burned to release energy or used for production of value added chemicals [23]. Gasification and combustion are the two closely related thermochemical process, but there is an important difference between them. Gasification packs energy in to chemical bonds in the product gas; combustion breaks those bonds to release the energy. The gasification process adds hydrogen to and strips carbon away from the hydrocarbon feedstock to produce gases with a high hydrogen-to-carbon ratio, while combustion oxidizes the hydrogen and carbon in to water and carbon dioxide, respectively. Biomass gasification process includes Drying, thermal decomposition or pyrolysis, partial decomposition of some gases, vapors, and char and gasification of decomposed products [23].

Pyrolysis is a thermal decomposition process that occur in the absence of any medium. Gasification, on the other hand, requires a gasifying medium like steam, air, or oxygen to rearrange the molecular structure of the feedstock in order to convert the solid feedstock into gases or liquids; it can also add hydrogen to the product. The use of medium is essential for the gasification process which is not the case for pyrolysis.

Biomass gasifier technologies are promoted in urban areas, especially in the areas where no grid connections are available. To utilize the biomass resources like rice husk, wood waste, agricultural waste, crop stalks etc. gasifier technologies are promo [24]. For power generation, biomass gasification technique consists of three major components; gasifier unit, gas production unit, internal combustion (IC) engine. Through this technique husk could be used as the source of electricity. In the first stage partial combustion of biomass to produce gas and char occurs along with generation of heat. This heat is utilized in drying of biomass to evaporate its moisture as well as for pyrolysis reactions to bring out volatile matter and provide heat energy necessary for further endothermic reduction reactions to produce producer gas which mainly consist of mixture of combustible gases such as CO (carbon monoxide),

hydrogen (H_2), traces of methane (CH_4) and other hydrocarbon. Normally air is used as gasifying agent, however use of oxygen can produce rich higher calorific value gas but due to cost implications is not usually preferred. The thermo-chemical conversion of solid coffee husk in the fluidized bed reactor into producer gas is called gasification and the process is shown in the figure below.

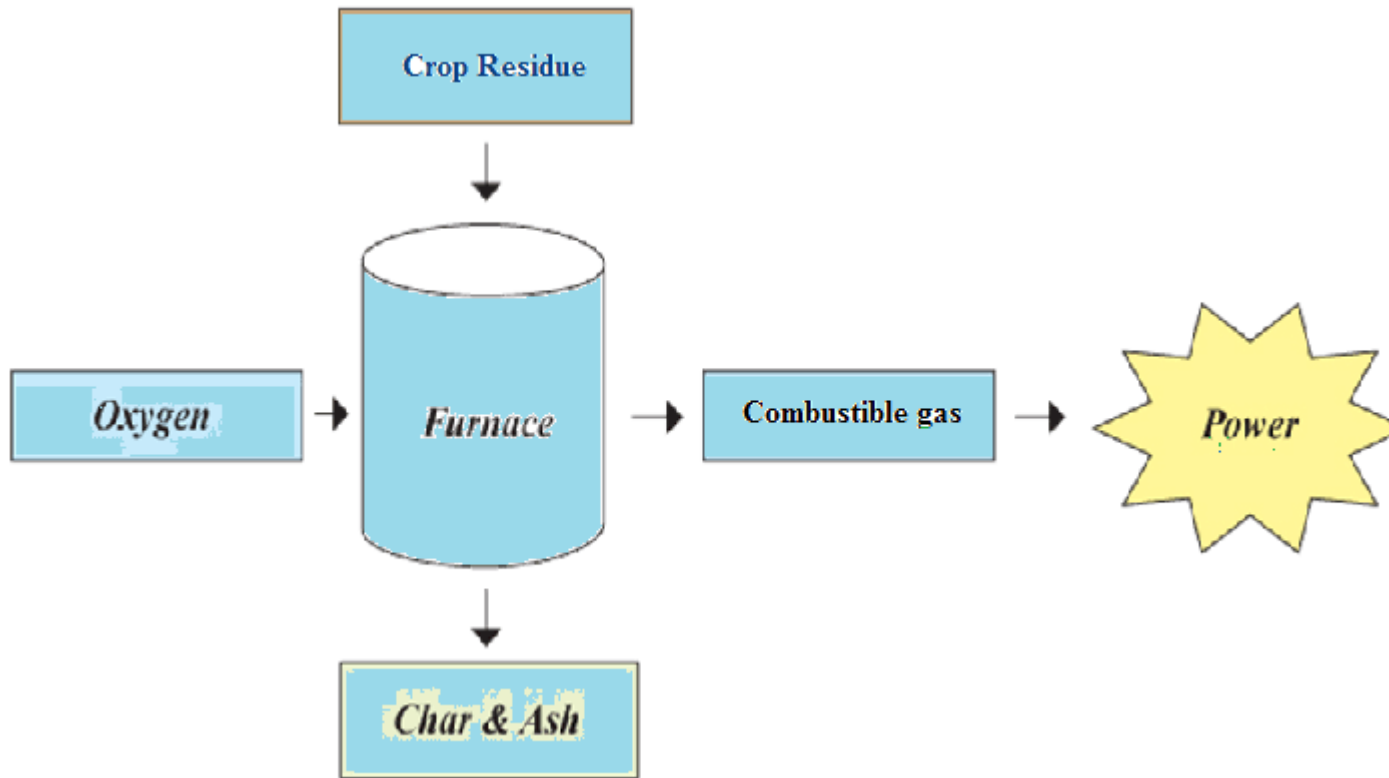


Figure 2.5: Gassification process [25]

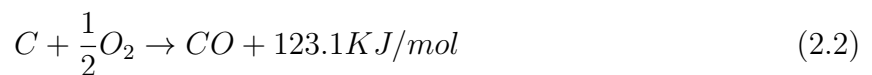
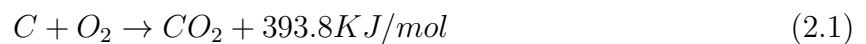
Reasons for selecting gasification technique:

1. relatively cheaper option for small scale industrial as well as power generation applications.
2. more efficient than traditional biomass utilization.
3. Environmental benefits as CO_2 gas is reduced.
4. Time Savings for Collection of Fuel.

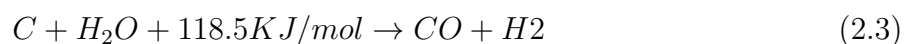
There are different types of reactors but fluidized type will be used because of the fast response to load.

B.Fluidized Bed Reactor :- in fluidized bed gasifiers the air is blown upwards through the biomass bed. The bed under such conditions behaves like boiling fluid and has excellent temperature uniformity and provides efficient contact between gaseous and solid phase. Generally the heat is transferred initially by hot bed of sand. The major advantage of fluidized bed gasifier over, say, downdraft is its flexibility with regard to feed rate and its composition.

Fluidized bed systems can also have high volumetric capacity and the temperature can be easily controlled [26]. Fluidization operations are based on contact between a fluid stream and a mixture of solid materials, which varies for each process. A packed bed is a column filled with packing materials. Liquid or gas can flow through a packed bed to achieve separations or reactions. In this experiment, we will see the interaction of particles and fluid. When a fluid, which can be liquid or gas, pass through the packing materials from bottom to top, there will be several regimes. **C.Fluidized bed-combustion features :-** a) direct contact of particles with intensive mass and heat exchange, b) uniform temperature in the fluidized bed, c) high heat capacity of fluidized bed making it possible to burn fuels of low quality, d) effectiveness of bed temperature control by supply of fuel, air and heat extraction. It is clearly seen how gas is produced from gasification of Biomass on the below schematic diagram. The biomass is fed through the feed door and is dried in the hopper. The nozzle is the channel through which limited amount of air goes in. **D.Gasification Reactions :-** The chemistry of biomass gasification is complex. Biomass gasification proceeds primarily via four distinct processes take place in a gasifier as the fuel makes its way to gasification. They are: a) Drying of fuel b) Pyrolysis a process in which tar and other volatiles are driven off c) Combustion d) Reduction. In complete combustion, carbon dioxide is obtained from the carbon and water from the Hydrogen. Oxygen from the fuel will of course be incorporated in the combustion products, Thereby decreasing the amount of combustion air needed [27]. Combustion, occurring in the oxidation zone, is described by the following chemical equations:



Thus, burning 1 mol or 12.01 g of carbon to carbon dioxide releases a heat quantity of 393.9KJ. These two reactions provide the heat necessary for the endothermic reactions in the drying, pyrolysis reaction zone. The water vapor introduced with the air production by the drying and pyrolysis of the biomass reacts with the hot carbon according to the following heterogeneous reversible water gas reaction:

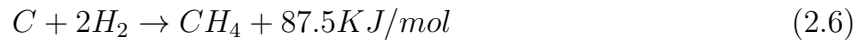
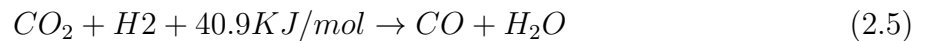


So, for each mol of carbon 118.5 KJ is consumed to produce one mol of CO and one mol of H₂.

The most important reduction reactions are the water gas reaction 2.3 and the following Boudouard reaction;



Besides these reactions several other reduction reactions take place of which the most important ones are the water shift reaction 2.5 and the methanisation reaction 2.6.



Equation 2.5 describes the homogenous water gas shift reaction.



The carbon or carbon monoxide may be combusted according to equations 2.7 and 2.8, although they produce heat which is beneficial to the gasification process, they are undesirable because they reduce the heating value. The ratio between of the concentration of carbon monoxide (CO) and water vapor (H₂O) and the concentration of carbon dioxide (CO₂) and (H₂) is fixed by the value of the water gas equilibrium constant (K_w).

$$Kw = ([CO] * [H_2O])/([CO_2] * [H_2]) \quad (2.9)$$

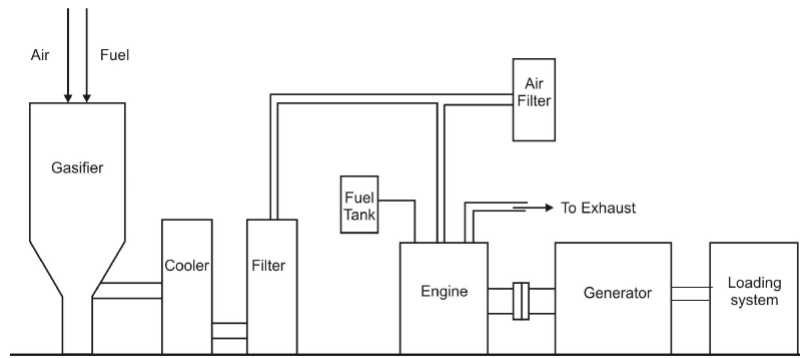


Figure 2.6: Biomass Power plant [23]

A gasifier fuel can be classified as good or bad according to the following parameters:-

A. Energy content and Bulk Density of fuel

The higher the energy content and bulk density of fuel, the similar is the gasifier volume since for one charge one can get power for longer time.

B. Moisture content

In most fuels there is very little choice in moisture content since it is determined by the type of fuel, its origin and treatment. It is desirable to use fuel with low moisture content because heat loss due to its evaporation before gasification is considerable and the heat budget of the gasification reaction is impaired. Besides impairing the gasifier heat budget, high moisture content also puts load on cooling and filtering equipment by increasing the pressure drop across these units because of condensing liquid. Thus in order to reduce the moisture content of fuel some pretreatment of fuel is required. Generally desirable moisture content for fuel should be less than 20%.

C. Dust content

All gasifier fuels produce dust. This dust is a nuisance since it can clog the internal combustion engine and hence has to be removed. The gasifier design should be such that it should not produce more than $2-6 \text{ g/m}^3$ of dust. The higher the dust produced, more load is put on filters necessitating their frequent flushing and increased maintenance.

D. Cleaning and cooling the producer gas

The temperature of gas coming out of generator is normally between $300 - 500^\circ\text{C}$. This gas has to be cooled in order to raise its energy density. Most coolers are gas to air heat exchangers where the cooling is done by free convection of air on the outside surface of heat exchanger. Since the gas also contains moisture and tar, some heat exchangers provide partial scrubbing of gas. Thus ideally the gas going to an internal combustion engine should be cooled to nearly ambient temperature. The gas generated in the reactor of a gasifier is

at a high temperature, and carries along with it some ash, besides its tar content, which are undesirable features, particularly when one needs to use the gas for applications such as running an internal combustion engine or a gas turbine. While tar can adhere to surfaces and cause jamming of moving parts and blockage of small passages, ash and other particulate matter would aggravate the problem. High temperature of the gas reduces the volumetric efficiency of an IC engine, since at these temperatures, since the density of the gas is low, the mass of gas-air mixture the cylinder can aspirate decreases, resulting in decrease in power output of the engine. This necessitates the cooling and cleaning of producer gas prior to its use. Cooling and cleaning is not as important in thermal applications as in the case of power generation applications. The Producer gas is then cleaned and cooled as it passes the cyclone and scrubber and delivered to the dual fuel engine as a clean gas through the main gas valve (MGV) while the diesel is supplied through the diesel tank.

Conventionally, dust removal from gases is effected by the use of cyclones, scrubbers or filters. Cyclones are effective when the gas flows at high velocity, and when particle sizes are larger than 15-20 microns. Scrubbers can serve a dual purpose of tar removal as well as particle removal. Filters can also serve this purpose, and it is necessary to replace the filter material periodically so as to prevent its clogging with tar. Commonly, all these three are used with gasifiers. Usually, more than one of these systems are used in series in most practical gasifiers in order to meet the cooling and cleaning requirements of the end use system.

E.Ash handling The mineral content in the fuel that remains in oxidized form after complete combustion is usually called ash. The ash content of a fuel and the ash composition have a major impact on trouble free operation of gasifier. Handling the ash is also very important and many times appears to be one of the technical barriers for biomass gasification. In this paper the ash from was used for fertilizer.

2.3 Syngas in Internal Combustion Engine

Syngas, an abbreviation for synthesis gas, is an end product of gasification. This is a name given for a mixture mainly comprised of CO and H₂ at varied proportions. It also consists of other gases like methane, nitrogen, and carbon dioxide apart from these major gases. It can be produced from different feedstock like coal, liquid hydrocarbons, biomass, and other waste products and the quality varies depending on the feedstock and the gasification process. The name syngas is a general term for any gasification product. However, different names were used for different products at different times in the past such as town gas, water gas, producer gas, and blast furnace gas [28]. Engines are divided into mobile and stationary

types depending on their applications. The engines used in stationary applications are of both internal and external combustion types while mobile type engines are only of internal combustion types. ICE is the most vital technological advancement, playing a major role in distributed energy power generation especially when there is a need for a variable power output. They have very flexible application in moving and nonmoving machineries. ICE is believed to have benefits like low capital cost, reliability, good part-load performance, high operating efficiency, and modularity and are quite safe to use as compared to other types of combustion technologies [29]. **Dual-fuel mode of operation** Application of syngas in diesel engines is considered to be a viable alternative both for the emissions and energy crises. However, syngas has high self-ignition temperature (typically above 500C) and as a result, it cannot be ignited by compression ignition in a diesel engine. A possible way of utilizing syngas in the CI engine is through dual fueling, where diesel is injected as a pilot fuel to initiate the ignition while syngas injected into the induction system. The main motivation in using syngas and other gaseous fuels in diesel engine is as a substitute to diesel as this can consequently reduce cost, minimize emissions (NO_x and particulate matters), and increase the engine performance.

2.4 Storage Battery

A battery is a device that stores direct current (dc) electrical energy in electrochemical form for later use. The amount of energy that will be stored or delivered from the battery is managed by the battery charge controller. Electrical energy is stored in a battery in electrochemical form and is the most widely used device for energy store in a variety of application. The conversion efficiency of batteries is not perfect. Energy is lost as heat and in the chemical reaction, during charging or recharging. Because not all batteries can be recharged they are divided in two groups. The first group is the primary batteries which only converts chemical energy to electrical energy and cannot be recharged. The second group is rechargeable batteries. Rechargeable batteries are used in hybrid power generation system. The internal component of a typical electrochemical cell has positive and negative electrodes plates with insulating separators and a chemical electrolyte in between. The cells store electrochemical energy at a low electrical potential, typically a few volts. The cell capacity, denoted by C, is measured in ampere-hours (Ah), meaning it can deliver C A for one hour or C*n A for n hours, [30]. Many types of batteries are available today, such as Lead-acid, Nickel cadmium, Nickel-metal, Lithium-ion, Lithium-polymer and Zinc air. Lead-acid rechargeable batteries continue to be the most used in energy storage applications

because of its maturity and high performance over cost ratio, even though it has the least energy density by weight and volume. These lead acid batteries come in many versions. The shallow-cycle version is the one used in automobiles, in which a short burst of energy is drawn from the battery to start the engine. The deep-cycle version, on the other hand, is suitable for repeated full charge and discharge cycles. Most energy storage applications require deep-cycle batteries. Depth of discharge is an important factor for the battery. It refers to how much capacity will be used from the battery. Most systems are designed for regular discharges of up to 40 to 80 percent. Battery life is directly related to how deep the battery is cycled. For example, if a battery is discharged to 50 percent every day, it will last about twice as long as if it is cycled to 80 percent [31]. The main factors affecting battery lifetime are grid corrosion, buckling of plates, sulfation, and stratification of the electrolytes. These factors are causing loss of active material and internal short circuits. If less active material is available, the ratio of the reaction components is becoming non-optimal, resulting in a drop of capacity and the charging efficiency is reduced. Internal short circuit leads to harmful deep discharge of the concerned cell and hence ruins the whole battery. Atmospheric temperature also affects the performance of batteries. Manufacturers generally rate their batteries at 25°C. The battery's capacity will decrease at lower temperatures and increase at higher temperature. The battery's life increases at lower temperature and decreases at higher. It is recommended to keep the battery's storage system at 25°C.

2.5 Hybrid Power System

A hybrid power system generally consists of renewable energy sources operating in parallel with a standby secondary source and storage units. A combination of different cooperating energy systems (which are complementary in nature) based on renewable energies, working with some back-up sources (like (LPG)/diesel/gasoline/biomass genset etc), is known as a hybrid power system [35]. **Hybrid power system configuration** In general, there are three types of hybrid power system configurations: DC coupled, AC coupled and Hybrid coupled System. **1. DC coupled configuration :-** in a dc-coupled configuration, shown in Figure 2.8, the different alternative energy sources are connected to a dc bus through appropriate power electronic (PE) interfacing circuits. The dc sources may be connected to the dc bus directly if appropriate. If there are any dc loads, they can also be connected to the dc bus directly, or through dc/dc converters, to achieve appropriate dc voltage for the dc loads. The system can supply power to the ac loads (50 or 60 Hz), or be interfaced to a utility grid through an inverter, which can be designed and controlled to allow bidirectional

power flow. The dc-coupling scheme is simple and no synchronization is needed to integrate the different energy sources, but it also has its own drawbacks. For instance, if the system inverter is out-of-service, then the whole system will not be able to supply ac power. To avoid this situation, it is possible to connect several inverters with lower power rating in parallel, in which case synchronization of the output voltage of the different inverters, or synchronization with the grid, if the system is grid-connected, is needed. A proper power sharing control scheme is also required to achieve a desired load distribution among the different inverters.

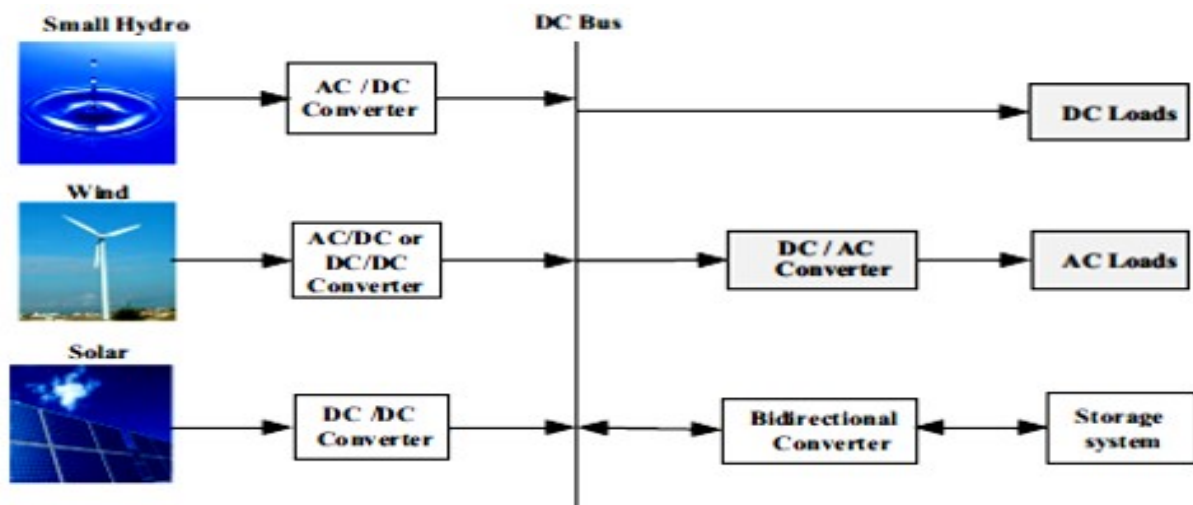


Figure 2.7: DC coupled Configuration [32]

2.AC Coupled Configuration :- In ac coupling the different energy sources are integrated through their own power electronic interfacing circuits to a power frequency ac bus. Coupling inductors may also be needed between the power electronic circuits and the ac bus to achieve desired power flow management. If dc power is needed it can be obtained through ac/dc rectification.

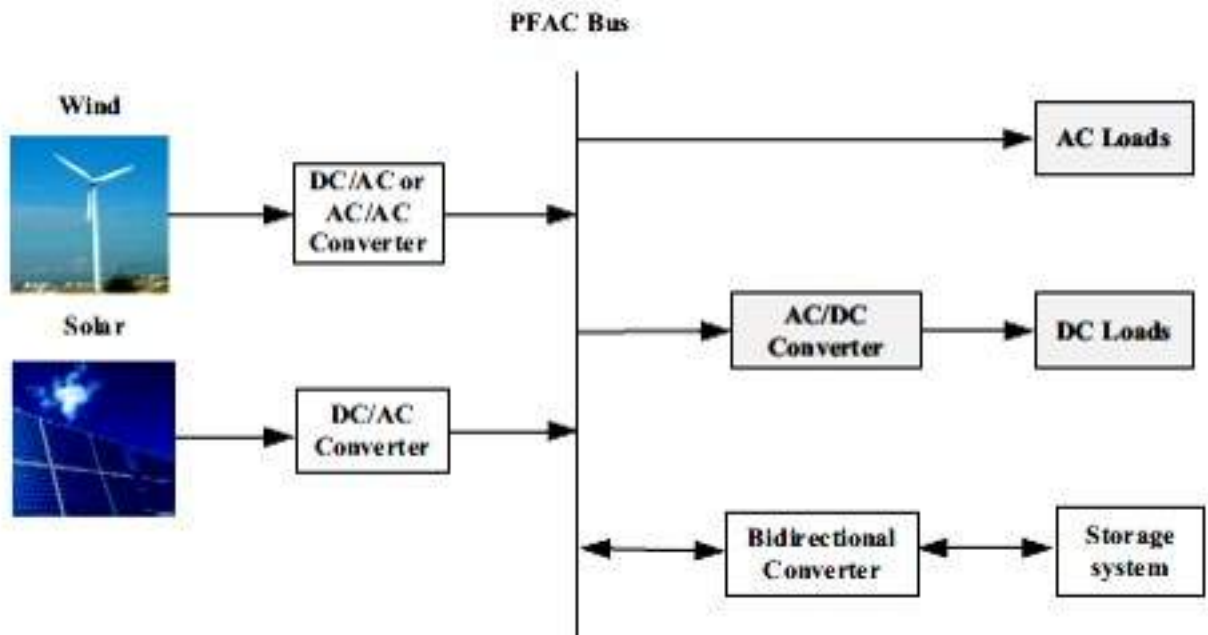


Figure 2.8: AC coupled Configuration [32]

3. Hybrid coupled configuration :- Instead of connecting all the distributed generation sources to just a single dc or ac bus, as discussed previously, the different distributed Generation sources can be connected to the dc or ac bus of the hybrid system. Figure 2.9 shows a hybrid-coupled system, where distributed generation resources are connected to the dc bus and/or ac bus. In this configuration, some energy sources can be integrated directly without extra interfacing circuits. As a result, the system can have higher energy efficiency and reduced cost. On the other hand, control and energy management might be more complicated than for the dc- and ac-coupled schemes. Different coupling schemes find their own appropriate applications. If major generation sources of a hybrid system generate dc power, and there are also substantial amounts of dc loads then a dc-coupled system may be a good choice. On the other and, if the main power sources generate ac (with reasonable power quality for the grid and the connected loads), then an ac-coupled system is a good option. If the major power sources of a hybrid system generate a mixture of ac and dc power, then a hybrid-coupled integration scheme may be considered.

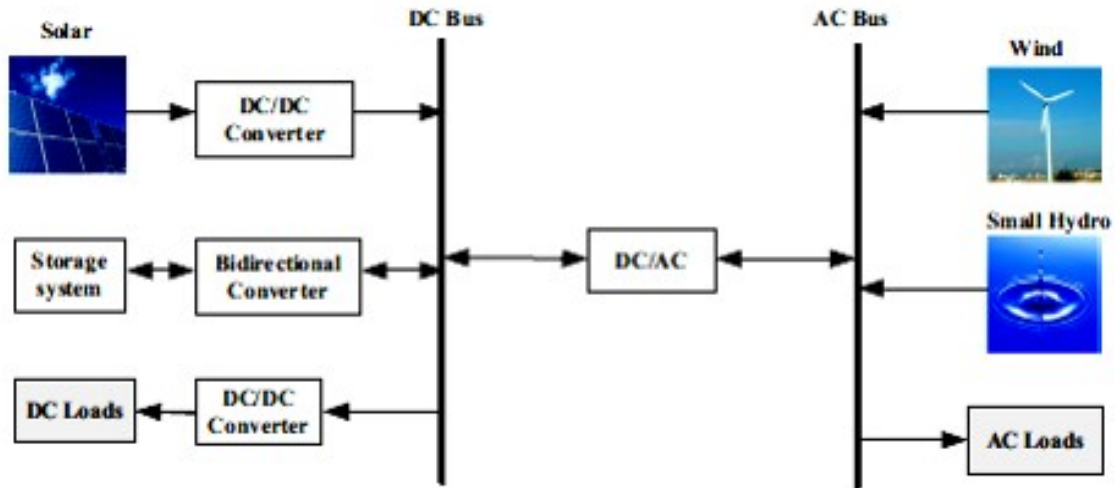


Figure 2.9: Hybrid coupled Configuration [32]

In hybrid configuration the amount of converters is reduced hence converter cost and conversion losses decreases. But has relatively complex control and energy management.

2.6 Fuzzy Logic Control

2.6.1 Introduction to fuzzy logic

Fuzzy logic is a super set of conventional (Boolean) logic that has been extended to handle the concept of partial truth. In the (Boolean) logic we see that the results for any operation can be true or false. If we refer to true by (1) and the false by (0) then the result may be (1) or (0) [33].

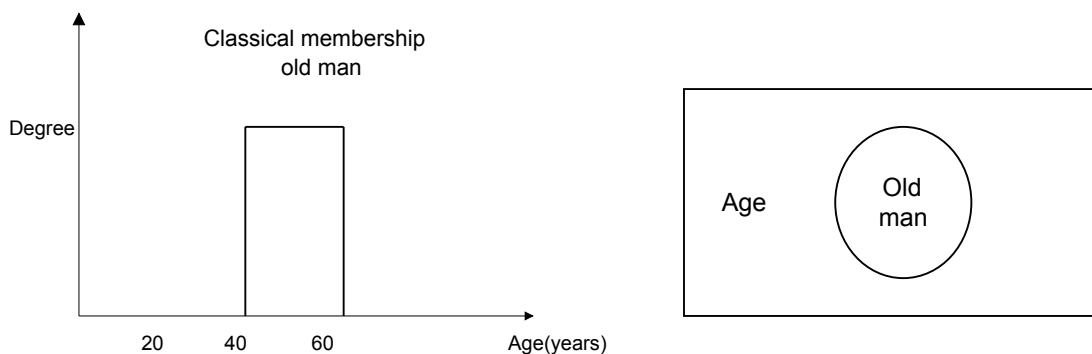


Figure 2.10: Classical sets [33]

Figure 2.10 shows an example for classical set, that has two values true or false. We see that the classical set have crisp boundary. And this example shows an age example: the man is old if he between 50 years and 60 years in that interval all age has the same degree (1). And outside of this interval, it has (0) degree. But there is problem, what about 49

years and 11 months, is the man young! No he old but has degree less than the 50 years, but in the Classical sets there are not degrees there are two values 1 or 0. So what is the solution, fuzzy sets give the solution [33]. **Fuzzy Set :-** Fuzzy sets are the sets, which do not have crisp [34] . There are not two values (true or false) but there are two limit is (1) completely true and the lower limit is (0) completely false and the result can have different degree between these limits.

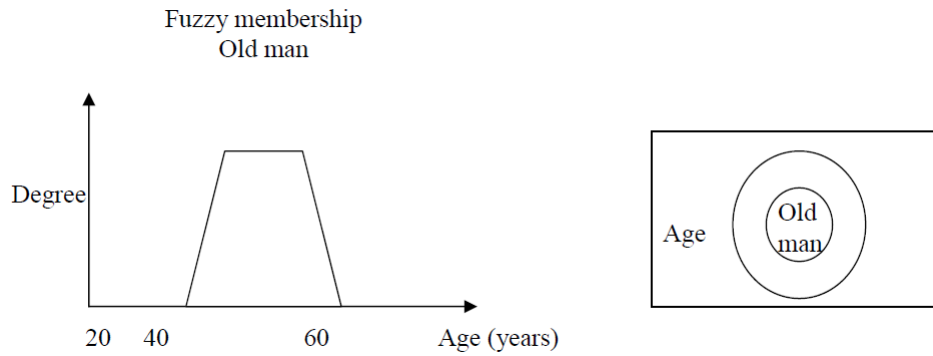


Figure 2.11: Fuzzy sets [34]

As shown in figure2.11a the ages between the interval (50, 60) have the same degree. But out this interval, the man is old but has different degree this set solve the problem of 49 years and 11 month. In Figure 2.11b we see two circles the small circle is (old man) set. Every element inside it has the same degree (1), and between the small circle and the big circle there are different degree of (old man), and every element outside the big cycle has the same degree (0). The next definition is the mathematically representation of fuzzy sets.

2.6.2 Membership Function

Fuzzy set can be represented by a membership function, that gives the degree of membership [35] as shown in figure 2.12.

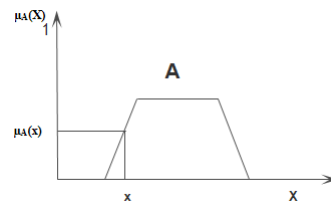


Figure 2.12: Membership Function [35]

In that Figure $\mu_A(x)$ in y-axis, is the symbol that refers to the degree of the membership function and $\mu(x)$ can be define as possibility function not probability function [35], and it takes value between (0,1). Anybody can ask what is the different between probability

function and possibility function. To answer this question let us see this example. If you and your friend went to visit another friend. And in the car your friend asks you, "Do you sure he is at the home?" and you answer "yes, I am sure but I do not know if he is in the bed room or on the roof ".You can give him another answer. You can answer him "I think 90% he is there". Look to the answer. In the first answer you are sure he is in the house but you do not know where he is in the house exactly. But in the second answer you are not sure he may be there and may be not there. That is the different between possibility and the probability in the possibility function the element is in the set by certain possibility and the probability in the possibility function the element is in the set by certain degree of, the probability function means that the element may be in the set or not . So if the probability of $(x) = 0.7$ that means (x) may be in the set by 70%. But in possibility if the possibility of (x) is 0.7 that means (x) is in the set and has degree 0.7. In the classical sets there is one type of membership function but in fuzzy sets there are different types of membership function, we now will show some of these types.

2.6.3 Linguistic Variable

Linguistic variable is an important concept in fuzzy logic [7].When fuzzy sets are used to solve the problem without analyzing the system; but the expression of the concepts and the knowledge of it in human communication are needed [34]. Human usually do not use mathematical expression but use the linguistic expression. For example, if you see heavy box and you want to move it, you will say, "I want strong motor to move this box" we see that, we use strong expression to describe the force that we need to move the box. In fuzzy sets we do The same thing we use linguistic variables to describe the fuzzy sets. These variable are words or sentence in natural or synthetic language [36]. For example if we take the universe U refer to the human age, we can take the interval between (50, 60) years and give it name "old man this name is called linguistic variable. We can use this name to refer to the set that contains the interval (50, 60) years. **Fuzzification:**-fuzzification means converting a crisp value of process variable into a fuzzy set. In order to make it compatible with the fuzzy set representation of the process state variable. Defuzzification: - Defuzzification strategy is aimed at producing a non-fuzzy control action, or we can say defuzzification means the conversion of the fuzzy output values into crisp values. There are different types of defuzzification methods.

1- Mean of Maximum method (MoM): In the Mean of Maximum (MoM) defuzzification method, the fuzzy logic controller first identifies the scaled membership function with the

greatest degree of membership. The fuzzy logic controller then determines the typical numerical value for that membership function. The typical numerical value is the mean of the numerical values corresponding to the degree of membership at which the membership function was scaled.

2- Center of Area (CoA): - The center-of-area (COA) method is the most popular defuzzification method

CHAPTER 3

POTENTIAL RESOURCE ASSESSMENT AND LOAD ESTIMATION

3.1 Overview of the selected site

Gumay woreda is found in the Jimma zone in Oromia Regional State and its geographical coordinates are 8 1' 0" North, 36 31' 0" East. Pera village is located in Gumay woreda. The village is found at 25 km from Toba the, capital of the woreda. Peoples living in this area are highly engage in farming and coffee production.

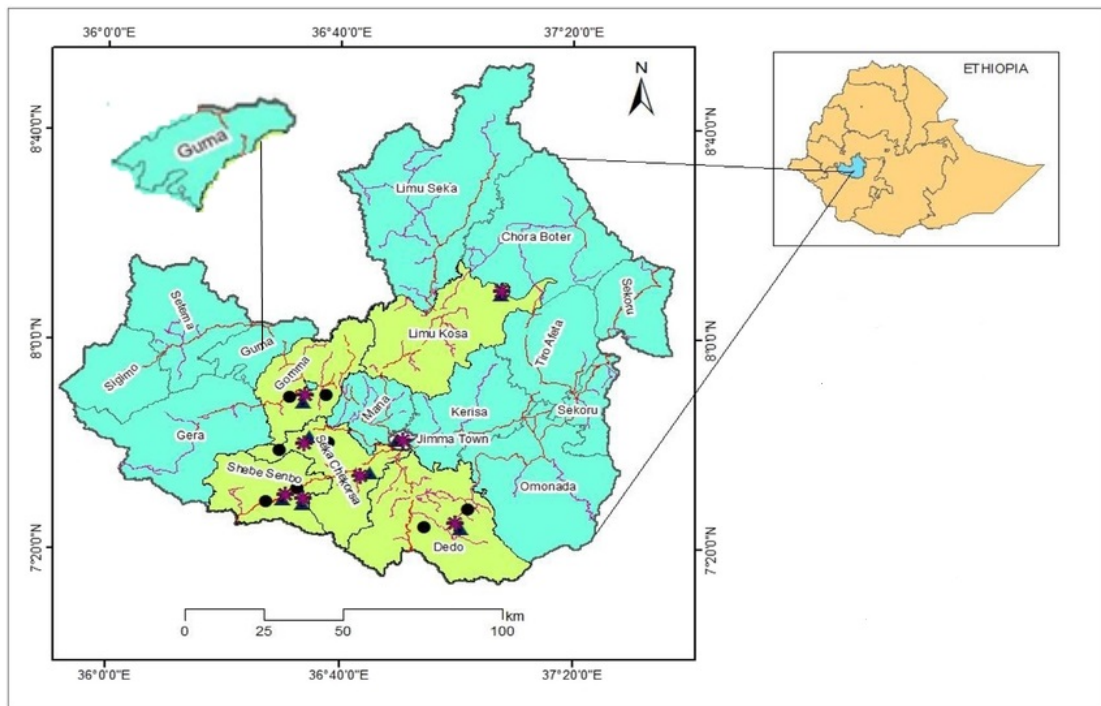


Figure 3.1: Map of Gumay,Jimma, Ethiopia [source:Google map]

3.2 Solar Energy potential assessment

The Solar duration data of Gumay woreda is obtained from office of Ethiopian National Metrology Agency of Jimma branch. The data obtained from NMA is the solar sunshine duration data from 2012 to 2015. Figure 3.2 shows monthly average solar duration data of Gumay Woreda.

Table 3.1: Monthly average of daily sunshine hour for Gumay[Source:NMA Jimma Branch

Month	Jan	Feb	Mar	Apr	May	June	July	Aug	Sep	Oct	Nov	Dec	
Av. of daily sunshine hour per year	2012	7.7	8.8	8.7	8.8	6.3	8	3.4	3.9	5.5	5.7	6.4	7.4
	2013	8.1	8.5	9.2	9	5.7	4.3	3.8	3.6	4.8	4.6	7.5	7.5
	2014	8.3	8.3	9.1	8.7	5.8	5.4	3.9	3.8	12.1	5.7	7.2	7.2
	2015	7.9	8.4	9	9.1	6.3	4.2	4.7	4.5	7.3	7	5.9	5.9
Monthly average of daily sunshine hour	8.00	8.50	9.00	8.90	6.03	5.48	3.95	3.95	7.43	5.75	6.75	7.00	

However the data of solar duration data is available, it is no longer used for modeling of PV system. Hence the solar duration data has to be converted to an appropriate solar radiation data. Figure shows monthly average solar sunshine duration data of Gumay woreda. However the data of solar duration data is available, it is no longer used for modeling of PV

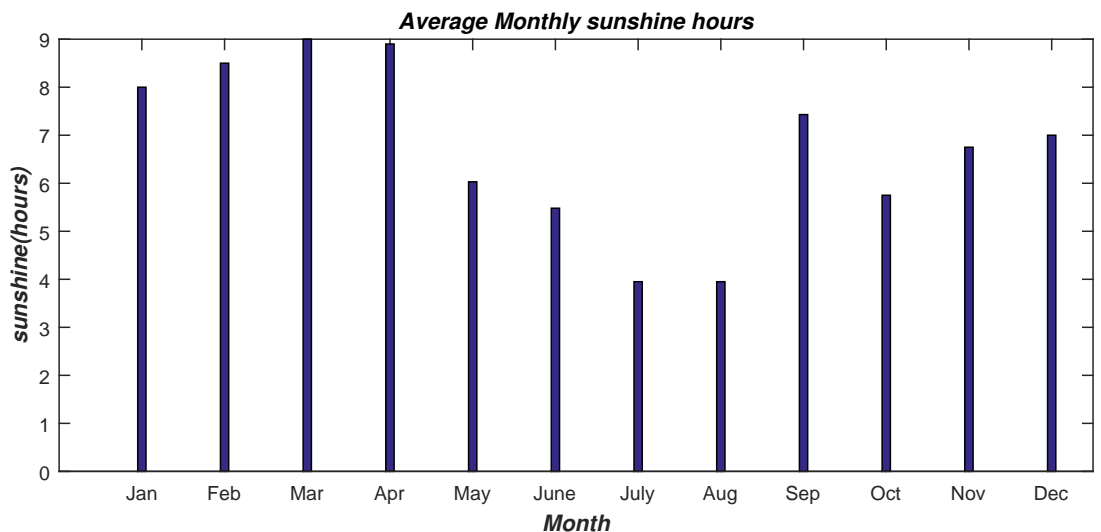


Figure 3.2: Average Monthly sunshine hour [Source: NMA, Jimma branch]

system. Hence the solar duration data has to be converted to an appropriate solar radiation data.

3.2.1 Solar insolation data and estimation

Radiation data are the best source of information for estimating average incident radiation. Lacking these data from nearby climatology offices, it is possible to use empirical relationships to estimate radiation from hours of sunshine or cloudiness. Although radiation from the suns surface is reasonably constant [37] [38], by the time it reaches the earths surface it is highly variable owing to absorption and scattering in the earths atmosphere. For Photovoltaic

system design it is necessary to estimate the insolation expected to fall on arbitrarily surfaces.

Sunshine hour data

A form in which solar insolation data are commonly available is as sunshine hours (SSH) [39]. This term indicates the number of daily hours of sunlight above a certain intensity, approximately 210 W/m², for a given period (usually a month), but gives no indication of absolute values and applies only to the direct component of sunlight.

For PV system design, the difficulty is in converting SSH data to a usable form. Here we consider techniques for estimating, from SSH data, the monthly average of daily global radiation incident on a horizontal surface [40].

$$H = \bar{H}_0 \left(a + b \frac{\bar{n}}{N} \right) \quad (3.1)$$

where H is the monthly average daily radiation on a horizontal surface (MJ/m²), \bar{H}_0 is the monthly average extraterrestrial radiation on a horizontal surface (MJ/m²), \bar{n} is the monthly average daily numbers of bright sunshine, N is the monthly average of the maximum possible daily hours of bright sunshine, a and b are regression constants extracted from measured data at various locations.

Extraterrestrial radiation

The total radiation emitted from the Sun results in an approximately fixed intensity of solar radiation outside the earth's atmosphere, because sun and the earth have a special relationship regarding distance [41]. Solar energy received, per unit time, on a unit area of surface perpendicular to the direction of propagation of the radiation at the earth's mean distance from the sun, outside the atmosphere, is called the solar constant generally denoted by G_{sc} . The solar radiation is disturbed by the earth's atmosphere i.e. some radiation are suppressed or attenuated by the atmosphere. Solar radiation available at the earth's surface in the absence of atmosphere is called the Extraterrestrial radiation, denoted as \bar{H}_0 . It can be calculated based on equation 3.2

$$H_0 = \frac{24 * 3600 * G_{sc}}{\pi} \left(1 + 0.033 \cos\left(\frac{360n_d}{365}\right) \right) * \left(\cos\Phi \cos\delta \sin\omega_s + \frac{\pi\omega_s}{180} \right) \sin\Phi \sin\delta \quad (3.2)$$

Where n_d is the day number starting from January 1st, G_{sc} is the solar constant with a generally accepted value of 1367 W/m², ϕ is the latitude of the location(⁰), δ is the declination angle(⁰).

Declination Angle

δ is the declination angle ($^{\circ}$), which is the angular position of the sun at solar noon, with respect to the plane of the equator. Generally Declination varies between -23.45° (on December 21) and $+23.45^{\circ}$ (on January 21) all over the world. Declination angle changes in every day throughout the year. Solar declination can be calculated with the help of Coopers equation [42].

$$\delta = 23.45 \sin\left(248 + n_d \left(\frac{360}{365}\right)\right) \quad (3.3)$$

Where n_d = day of the year ($n_d = 1, 2, 365$) (For 1^{st} Jan, $n_d=1$, 1^{st} Feb, $n_d=32$).

Solar Hour Angle (ω)

The Solar Hour angle (ω) is the angular displacement of the Sun east or west with respect to the local meridian throughout the day [9]. Solar hour angle is zero at the solar noon because at that time Sun's position and local meridian are at the same line. In the morning, the solar hour angle is negative and in the afternoon it is positive. Solar hour angle varies 15° per hour. At 6 am, the solar hour angle is -90° . In the next hour it will be -75° ($-90+15=-75$). It can be calculated from equation 3.4 [9].

$$\sin\omega = \frac{\sin\alpha - \sin\delta\sin\phi}{\cos\delta\cos\phi} \quad (3.4)$$

Table 3.2: Solar Hour angle of a day

6am	7am	8am	9am	10am	11am	12noon	1pm	2pm	3pm	4pm	5pm	6pm
-90	-75	-60	-45	-30	-15	0	15	30	45	90		

Sunset hour angle (ω_s)

The sunset hour angle is the solar hour angle at a particular time i.e. the time when the sun sets. Sunset hour angle changes throughout the year as the solar time of sunsets are changing day wise. Solar hour angle at the sunrise is numerically equal to the sunset angle. Sunset hour angle is dependent on declination and it can be calculated as follows (equation 3.5) [9].

$$\cos\omega_s = -\tan\phi \tan\delta \Rightarrow \omega_s = \cos^{-1}(-\tan\phi \tan\delta) \quad (3.5)$$

The sunset hour always expressed in radian. Hence equation (3.6) is used to convert the sunset obtained in degree to radian. The available sunshine hour data from the National Meteorological Agency of Ethiopia (Jimma branch) was used to estimate the solar radiation energy of the sites.

$$N_s = \frac{2}{15} * \omega_s \quad (3.6)$$

where N_s is the sun set hour in radian. The accuracy of the estimated values of the regression coefficients a and b are expected to improve by adding the effect of elevation, sunshine duration, and latitude together. Thus the regression coefficients a and b in terms of the latitude, elevation and percentage of possible sunshine for any location around the World (for $5 < \phi < 54$) are correlated by

$$a = -0.309 + 0.539 \cos \phi - 0.0693h + 0.290\left(\frac{n}{N}\right) \tag{3.7}$$

$$b = 1.527 - 1.027 \cos \phi + 0.092h - 0.359\left(\frac{n}{N}\right) \tag{3.8}$$

where, h, is Altitude of a site in kilometers (1740m for the specific study site) δ , is declination angle for the average day in the month (calculated from the above equation 3.3) ϕ , is Latitude of the site (8.0167) ω_s , Sunset hour angle (calculated from the above equation 3.6)

Table 3.3: Monthly solar radiation at the study site

Mid of month	n_d	δ	ω	N	n	n/N	a	b	H_o (KWH/ m^2)	H (KWH/ m^2)	NASA
January	15	-23.05	86.56	11.54	8	0.69	0.31	0.42	9	5.39	5.86
February	45	-22.17	86.71	11.56	8.5	0.74	0.32	0.41	9.02	5.58	6.24
march	75	-15.52	87.76	11.70	9	0.77	0.33	0.4	9.54	6.03	6.21
April	105	-4.81	89.32	11.91	8.9	0.75	0.32	0.4	10.13	6.32	6.13
May	135	7.15	91.01	12.13	5.8	0.48	0.24	0.5	10.41	5.02	5.63
June	166	17.52	92.55	12.34	5.6	0.45	0.24	0.51	10.32	4.82	5.11
July	197	23.01	93.43	12.46	4.5	0.36	0.21	0.54	10.19	4.13	4.65
August	227	22.24	93.30	12.44	4.6	0.37	0.21	0.54	10.3	4.24	4.78
September	258	15.36	92.22	12.30	7.5	0.61	0.28	0.45	10.59	5.91	5.43
October	289	4.22	90.59	12.08	6.6	0.55	0.26	0.48	10.67	5.58	5.64
November	319	-7.72	88.91	11.85	7.6	0.64	0.29	0.44	10.27	5.9	5.6
December	350	-17.91	87.39	11.65	8	0.69	0.3	0.43	9.53	5.68	5.76
Average										5.38	5.59

By using equation 3.1 to equations 3.8 the solar radiation data of Gumay woreda is found and given in figure shown below.

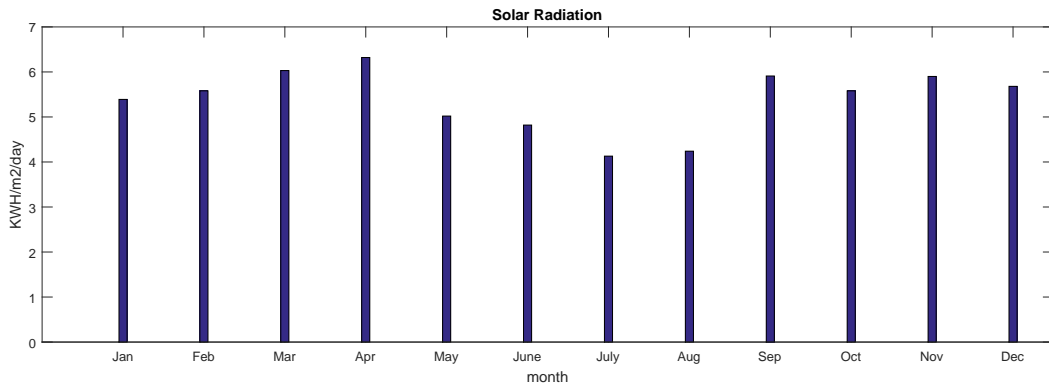


Figure 3.3: Solar Radiation of Gumay worda[source:Author of thesis]

3.2.2 Data Comparison of Global solar radiation of NMA and NASA

In order to make sure that the data obtained from NMA was valid, the sunshine hour obtained from NMA processed and compared with NASA data. as shown in table3.4 and in fig3.4 the average global solar radiation of NMA was 5.38 KWH/m²/day and the average global solar radiation of NASA was 5.59 KWH/m²/day. The average difference between the calculated and NASA was 0.2 KWH/m²/day. This shows that the data obtained from NMA was valid and there was enough data to electrify the village using solar system.

Table 3.4: Data Comparison

Month	Jan	Feb	Mar	Apr	May	Jun	Jul	Aug	Sep	Oct	Nov	Dec	Ave
NMA	5.39	5.58	6.03	6.32	5.02	4.82	4.13	4.24	5.91	5.58	5.9	5.68	5.38
NASA	5.86	6.24	6.21	6.13	5.63	5.11	4.65	4.78	5.43	5.64	5.6	5.76	5.59
change	-0.47	-0.66	-0.18	0.19	-0.6	-0.29	-0.52	-0.54	0.48	-0.06	0.3	-0.08	-0.2

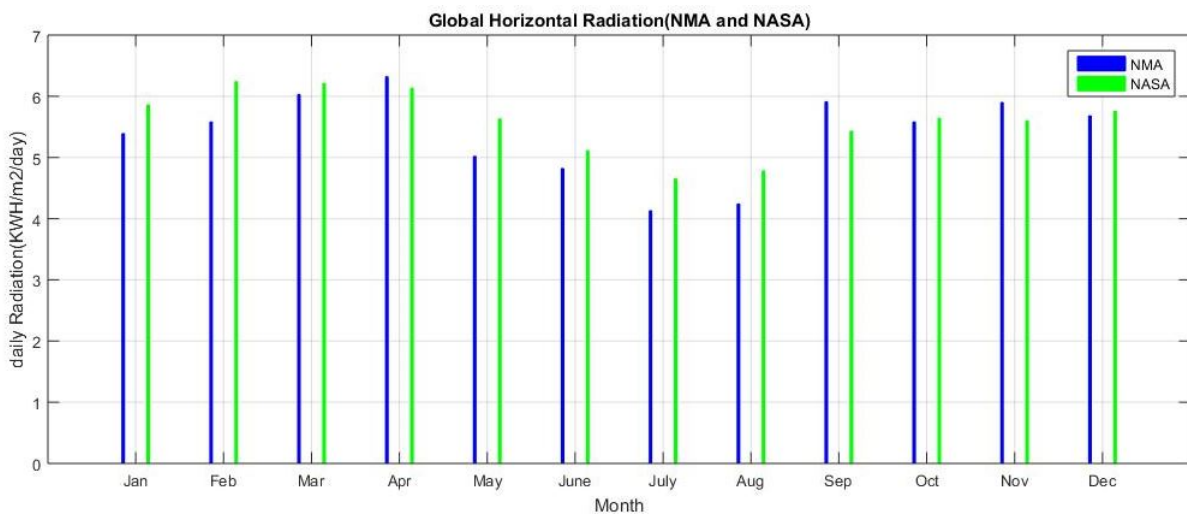


Figure 3.4: Data Comparison of NMA and NASA [source:Author of thesis]

3.3 Bio-mass Energy resource

About 25% of the Ethiopian populations directly or indirectly deriving their livelihoods from coffee [25]. As an agricultural country, Ethiopia produces considerable amount of biomass each year. Most of biomass has been utilized for domestic energy purpose, mainly by direct combustion (which converts solid biomass into heat). On the contrary, coffee husk from coffee processing industries is not used as a fuel in most cases due to the poor handling of coffee husk to be used as domestic fuel. However, gasification, which converts solid biomass into fuel gas containing CO and H_2 or so-called synthesis gas, has to be considered as a promising alternative owing to a number of advantages. Annual export and Domestic use of coffee of Gummay Wereda for 10 years are listed in the table below.

Table 3.5: Average yearly coffee Production

Year(E.c)	Washed(metric ton)	Unwashed(metric ton)	Total production(metric ton)
1998	156	1657	1813
1999	130	1560	1690
2000	213	1756	1969
2001	146	1825	1971
2002	136.99	1036.25	1173.24
2003	416.8	1895.4	2312.2
2004	70.86	2027.25	2098.11
2005	216	1817.5	2033.5
2006	148.3	1450	1598.3
2007	258.58	1533.16	1791.74
Average Yearly Production	189.253	1655.756	1845.009

The above table shows the annual coffee production of Gumay woreda which is also indicated in bar graph shown below. The total average annual coffee production of Gummay woreda is 1845.009 metric tons per year. Experimental researches highlights and defines clearly that the coffee seed to coffee husk ratio is 52%: 48%, then accordingly 1845.009 metric tons of coffee seed and 1703.08523 metric tons of coffee husk has been produced from 3548.0942 metric tons of coffee fruit.If 30% of coffee husk produced is assumed to be wasted, the rest 70% (1,192.16 metric tons) which is 3.3 metric tons per day of the produced husk is dumped (thrown) without any economic value to environment more over this will a national waste and pollution, hence must be clearly utilized, this research papers clearly incorporate the efficient usage of the above resource.

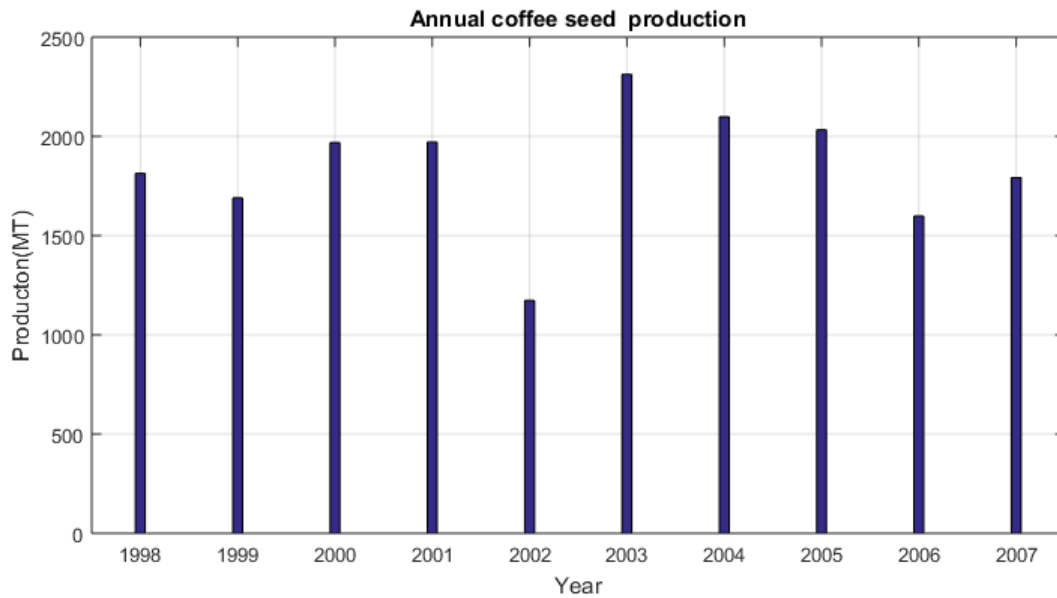


Figure 3.5: Average Yearly coffee seed production [source:Author of thesis]

3.4 Load Estimation

According to Getachew Bekele [8], electric load in the rural villages of Ethiopia can be assumed to be composed of lighting, radio and television, water pumps, health post and primary schools load. Tamrat [43] considered only lighting, radio and television as a community load. In this study, electricity for lighting, radio, Electric Stove and television, water pumps, Communal load, health post and primary schools load are considered.

Household Loads:- In this thesis, the energy demand for 1000 peoples or 200 households, which are leaving without electricity now or even in the near future are considered. Each household is to be installed with four CFLs of 5W rating to be lit from 18 : 00 to 23 : 00. Additionally it is also assumed that students in each household do self-learning during night time and for this purpose they use one 5W rating CFL lamp for 4 hours. Further, it is assumed that 100% of the population are using energy for lighting and radio, 60% of the households are used for TV, 50% of the households are used a 1KW electric stove for one hour and 100% are used for radio set. Communal loads is also considered for two cafeterias consisting of TV, Stove, Coffee maker, Cattle and lighting loads. Generally, the necessary step to estimate how much electricity required in the study is list all electrical appliances, estimate how long they are used, put the power that each appliance consumes, for each appliance; multiply the power rating in watts by the number of hours used each day to obtain the number of watt hours that the appliance used per day and add up the watt hours for all appliances. Thus the total energy consumption of house hold loads, primary school loads, health center load are tabulated in table 3.6 and table 3.7.

Table 3.6: Energy Consumption of Household

Time segment	lighting(4KW)	stove(50KW)	Radio(1KW)	TV(8.4KW)	communal load 2cafe					Total(KWH)
					TV(140w)	coffee maker(2KW)	Kettle(2.4KW)	lighting(70W)	stove(2kw)	
00:00-01:00										0.00
01:00-02:00										0.00
03:00-04:00										0.00
04:00-05:00	1000									1.00
05:00-06:00	1000									1.00
06:00-07:00		25000	1000		140	1000	4800	70	4000	36.01
07:00-08:00			1000	8400	140	1000			4000	14.54
08:00-09:00			1000		140	1000			2000	4.14
09:00-10:00			1000		140	1000			2000	4.14
10:00-11:00					140	2000			4000	6.14
11:00-12:00		25000			140	2000			4000	31.14
12:00-13:00					140				2000	2.14
13:00-14:00				8400	140				2000	10.54
14:00-15:00					140	2000	4800		4000	10.94
15:00-16:00					140	2000			4000	6.14
16:00-17:00					140	2000			4000	6.14
17:00-18:00		25000	1000		140					26.14
18:00-19:00	4000		1000		140			70		5.21
19:00-20:00	4000	25000	1000	8400	140			70		38.61
20:00-21:00	4000		1000	8400	140			70		13.61
21:00-22:00	4000			8400				70		12.47
22:00-23:00	1000									1.00
23:00-00:00	1000									1.00
Total daily load	20000	100000	8000	42000	2100	14000	9600	350	36000	232.05

Primary School, Health Center and Industrial Loads :- in load analysis of the community the load of one elementary school and one health center is also considered. Accordingly the primary school consists of eight classrooms and the classroom will be installed with three 5W CFLs (compact fluorescent lamps) and a 5w radio receiver. Additional four CFLs (of 5W) for external lighting are also considered. Similarly for the health centers, having three rooms, one 5W CFL per room and two 5W CFL for external lighting are considered. A vaccine refrigerator of 80W working for 24h; a 20W capacity microscope and a

70W TV set and a 5W radio for the office hours; and a 1kW water heater operational for 3h per day are also suggested for each health centers. Water pumping system is required for the households, the schools and health care centers. A minimum of 100l of water per day per family and 2400l/day for each pair of one health center and one primary school is suggested [44]. To accomplish this, two pump of 450W (with a capacity of 30l/m) operating for 5h/day are to be installed to supply water for the community. Another 2 pumps of 150W (with a capacity of 10l/m) for the primary schools and health centers operating for 4h/day are assumed. A 150w Coffee washer working 8 hours per day is also considered as an industrial load.

Table 3.7: Energy Consumption of primary school and health center

Time segment	school load		Health center load						industrial load			total(KWH/day)
	lighting(120W)	Radio(40W)	TV(70w)	Radio(5W)	lighting(25W)	Refrigerator(80W)	microscope(20W)	Water heater(1KW)	water pump(900W)	water pump(300W)	Coffee washer(150W)	
00:00-01:00		5		5		80		Water	water pump(900W)	water pump(300W)	Coffee	0.09
01:00-02:00		5		5		80						0.09
03:00-04:00		5		5		80						0.09
04:00-05:00		5		5		80						0.09
05:00-06:00		5		5		80						0.09
06:00-07:00				5		80						0.09
07:00-08:00				5		80						0.09
08:00-09:00		40	70			80	20				150	0.36
09:00-10:00		40	70			80	20				150	0.36
10:00-11:00		40	70			80	20		900	300	150	1.56
11:00-12:00		40	70			80	20	1000	900	300	150	2.56
12:00-13:00			70			80		1000	900	300		2.35
13:00-14:00		40	70			80	20	1000	900	300	150	2.56
14:00-15:00		40	70			80	20		900		150	1.26
15:00-16:00		40	70			80	20				150	0.36
16:00-17:00		40	70			80	20				150	0.36
17:00-18:00		5	70			80						0.16
18:00-19:00	120	5		5	25	80						0.24
19:00-20:00	120	5		5	25	80						0.24
20:00-21:00	120	5		5	25	80						0.24
21:00-22:00		5		5		80						0.09
22:00-23:00		5		5		80						0.09
23:00-00:00		5		5		80						0.09
Total daily load	360	5	700	65	75	1840	160	3000	4500	1200	1200	13.11

Based on the above analysis the total energy consumption of the community is $245.16KWh/day$.

The annual energy consumption of this village becomes $89,483.4KWh$ which is obtained by multiplying the daily energy consumption by 365. The average load demand per hour becomes $10.215KW$, which is found by dividing the annual energy consumption by 8760 hours. From the analysis the peak load of the village becomes $38.845KW$. So, the average load factor of this system becomes 26.29% which is found by dividing the average load with the peak demand of the village. Now the installed capacity of the system is found as peak load

plus loss of the system.

$Installed\ capacity = peak\ load + loss, \text{ assume } 10\% \text{ of loss}$

$Installed\ capacity = 38.45\text{KW} + 3.845\text{KW} = 42.295$. Which is approximated to 43KW . The average hourly load demand curve is shown figure 3.6.

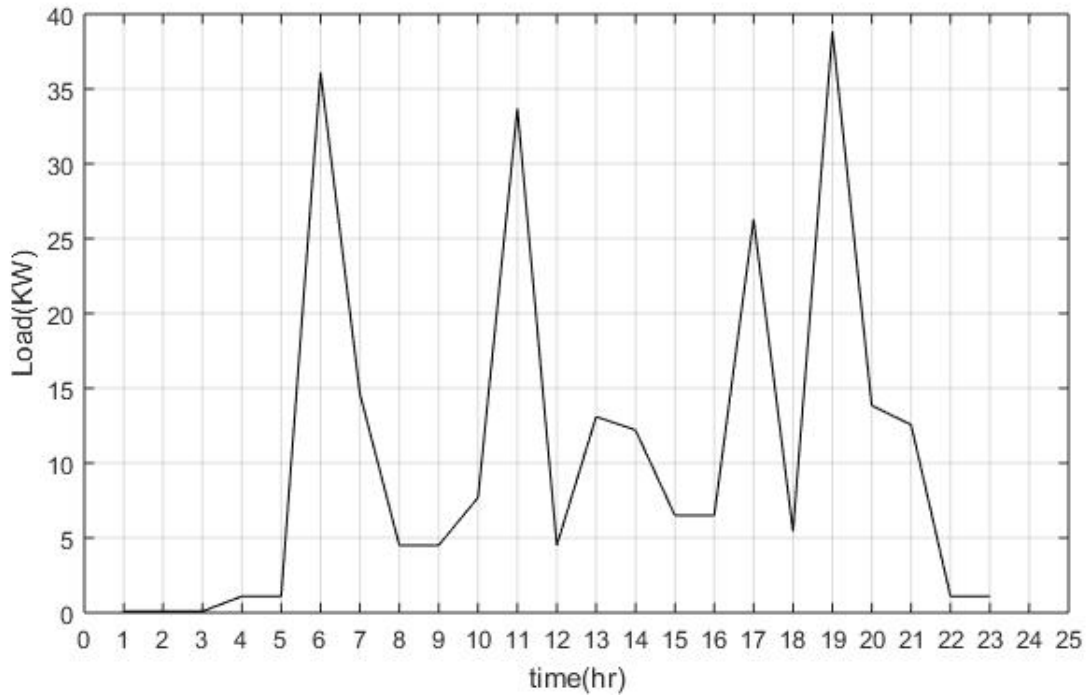


Figure 3.6: Daily Load Curve of Pera [source:Author of thesis]

CHAPTER 4

MODELING, SIMULATION AND COST ESTIMATION OF HYBRID POWER SYSTEM

4.1 Proposed Hybrid system

In this Section, the combination of renewable energy technologies for generating electricity that suitable to Pera village will be discussed. The load demand of Pera and the potential renewable energy resources have been already known. The suitable renewable energy technologies that can be applied to that village are biomass Gasification, and photovoltaic with storage Batteries. The schematic of the system can be seen as Figure 4.1.

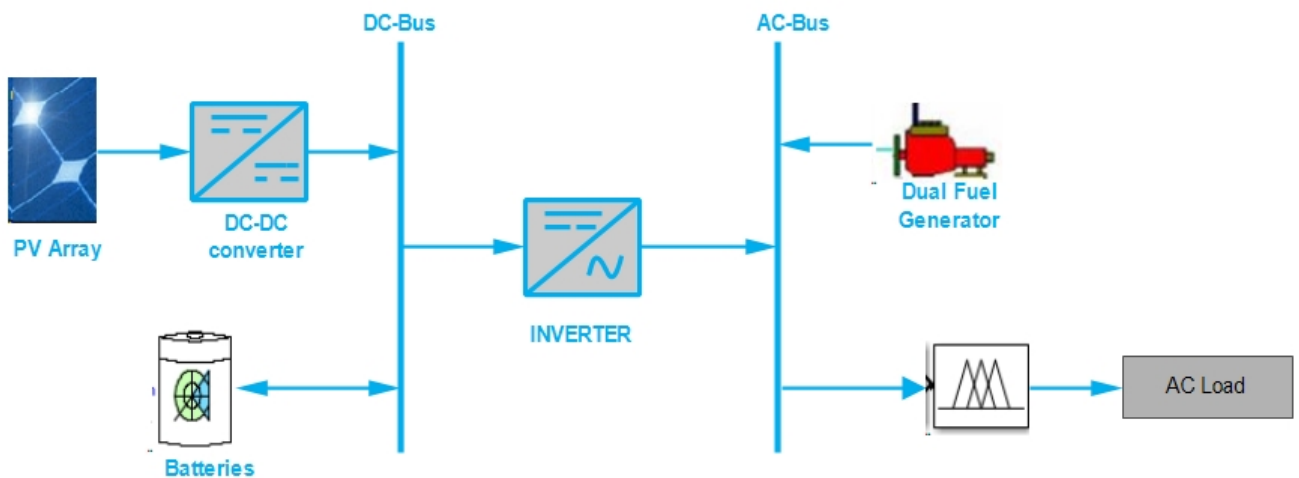


Figure 4.1: proposed Hybrid system[source:Author of thesis]

As shown in the figure the proposed hybrid system consists of PV system, Dual fuel generator and storage Batteries. Now, let us see the Design and Modeling of each system.

4.2 Modeling and Designing of PV system

4.2.1 PV system Designing and Sizing

In order to size the solar panel the first step is to determine the total energy demand per day. Since the system is a hybrid system the solar panel contribution is 17.4% of the energy demand per day. From the load demand data analysis result, the solar power contribution is 42.66 kilo watt hour per day. From the selected high multi crystalline KYOCERA KC200GT PV module given in Annex (A), max power voltage at STC is 26.6 and the Selected PV module guaranteed power output at STC is 200 watts. Table 4.1 below shows data sheet of the selected PV module.

Table 4.1: Electrical specification for KC200GT panel

KC200GT solar panel Specifications	
Maximum Power	200W
Voltage @Pmax	26.3V
Current @Pmax	7.61A
Open Circuit Voltage	32.9V
Short Circuit Current	8.91A

PV system sizing :- since the PV system is hybridized with the biomass system, the contribution of the PV system is 17.4% of the demand per day. The Solar panel contribution is 42.66Kwh/day. By selection the system voltage as 48 V.

$$LoadinAH = \frac{42.66Kwh}{48V} = 888.7Ah \quad (4.1)$$

Module size :- required power from solar array

$$P_{required} = L * C_f \quad (4.2)$$

Where, L- is Load in Ah and L_f is the safety factor due to losses and accommodation dust on the module. Therefore,

$$P_{required} = 888.7Ah * 1.3 = 1155.32Ah/day \quad (4.3)$$

Power generated from the module in Ah

$$P_g = \frac{200w}{26.3V} * 3.95hr/day = 30.04Ah \quad (4.4)$$

Then, total number of PV module required to generate the required power

$$N = \frac{P_{required}}{P_g} = \frac{1155.32Ah}{30.04Ah} = 38.45 = 40 \quad (4.5)$$

From the selected solar panel

$$NumberofPVstringsinseries = \frac{systemvoltage}{PVvoltage} = \frac{48}{24} = 2 \quad (4.6)$$

$$\text{Number of panels connected in parallel} = \frac{\text{number of total panel}}{\text{number of panels connedinseries}} = \frac{40}{2} = 20 \quad (4.7)$$

4.2.2 Equivalent circuit and Mathematical modeling of PV system

The behavior of photovoltaic (PV) cells can be modeled with an equivalent circuit shown in Figure 4.2 [41]. This circuit includes a series resistance and a diode in parallel with a shunt resistance. The letter V represents the voltage at the load. This circuit can be used for an individual cell, for a module consisting of several cells, or for an array consisting of several modules.

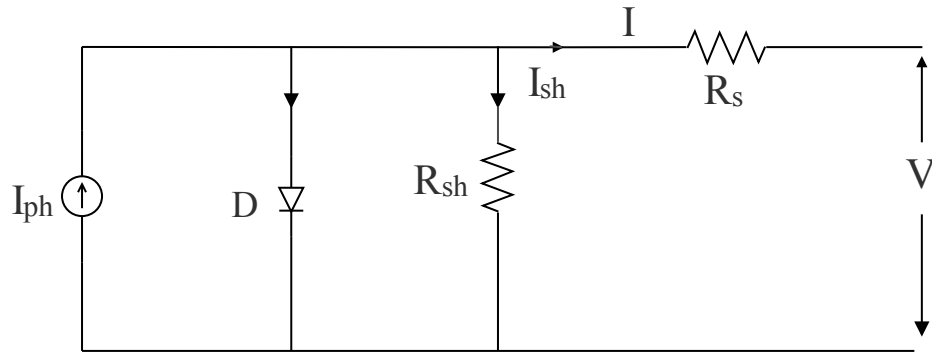


Figure 4.2: Equivalent circuit of single solar cell [41]

Application of Kirchoffs Current Law on the equivalent circuit results in the current flowing to the load

$$I = I_{ph} - I_d - I_{sh} \quad (4.8)$$

The current through the diode can be calculated as follows.

$$I_d = I_0 \left(e^{\frac{V_d}{V_T}} - 1 \right) \quad (4.9)$$

$$V_d = V + I * R_s \quad (4.10)$$

$$V_T = \frac{nKT}{q} \quad (4.11)$$

$$I_{sh} = \frac{V_d}{R_{sh}} = \frac{V + I * R_s}{R_{sh}} \quad (4.12)$$

By substituting equations 4.9 to 4.12 in equation 4.8 the current flowing in to the load can be expressed as follows.

$$I = I_{ph} - I_0 \left(e^{\frac{q(V+I*R_s)}{nKT}} - 1 \right) - \frac{V + I * R_s}{R_{sh}} \quad (4.13)$$

Where, n : ideality factor I_{ph} : light current I_0 : diode reverse saturation current R_s : series resistance R_{sh} : shunt resistance K : Boltzmann constant [$1.38*10^{-23}$ J/K] T_c : is absolute temperature of cell q : charge of electron [1.602×10^{-19} C] A solar cell can be characterized by the following fundamental parameters.

(a) short circuit current(I_{sc}):When the voltage across the solar cell is zero or the solar cell is short circuited, the current flow through the cell at that time is called the short circuit current current(I_{sc}) [45]. It depends on a number of factors such as Solar cell area, optical properties, efficiency of light intensity, the spectrum of the incident light etc. To avoid the complexities, the short circuit current is considered to be equal with the photo current (Ip). This photo current is directly proportional to the solar irradiance, G (W/m²). But this assumption leads some deviation from the actual output of PV module. So an exponent , is considered to look after all the non-linear effects due to photocurrent .The temperature dependence of short circuit current is very little.

(b) open circuit voltage(Voc):Open circuit voltage is the maximum available output voltage from a solar cell when the total current through the device is zero [45]. Basically solar cell consists of a P-N junction diode circuit. So with the increase in temperature the saturation current increases exponentially, as a result, Voc maintains an exponential relationship with the temperature [46]. This assumption causes some deviation from the accurate performance. To compensate that some other parameters like shunt resistance, series resistance and the non-ideality of the diode have to be considered.

(c) Fill Factor(FF):Fill factor is the measure of squareness of solar cell [45]. FF is a parameter which determines the maximum power output from a solar cell with the help of short circuit current and open circuit voltage. The maximum current and maximum voltage of a solar cell is the short circuit current and open circuit voltage respectively. The FF can be defined as the ratio of the maximum power from the solar cell to the product of open circuit voltage (Voc) and short circuit current (Isc) [47]. The parasitic resistances of

PV-panel, both in series and shunt, try to reduce the value of Fill Factor.

4.3 MATLAB Modeling of PV system

The name MATLAB stands for MATrix LABoratory. MATLAB was written originally to provide easy access to matrix software developed by the LINPACK (linear system package) and EISPACK (Eigen system package) projects. MATLAB is a high-performance language for technical computing. It integrates computation, visualization, and programming environment. Furthermore, MATLAB is a modern programming language environment: it has sophisticated data structures, contains built-in editing and debugging tools, and supports object-oriented programming. These factors make MATLAB an excellent tool for teaching and research. **Simulink** is a graphical extension to MATLAB for modeling and simulation of systems. In Simulink, systems are drawn on screen as block diagrams. Many elements of block diagrams are available, such as transfer functions, summing junctions, etc., as well as virtual input and output devices such as function generators and oscilloscopes. Simulink is integrated with MATLAB and data can be easily transferred between the programs. Simulink is supported on UNIX, Macintosh, and Windows environments; and is included in the student version of MATLAB for personal computers. MATLAB2015a is an extended version of MATLAB2014b. The design is performed using the PV array which is found in MATLAB2015a library. The PV Array model provided in MATLAB2015A is used for this thesis as shown in figure 4.3.

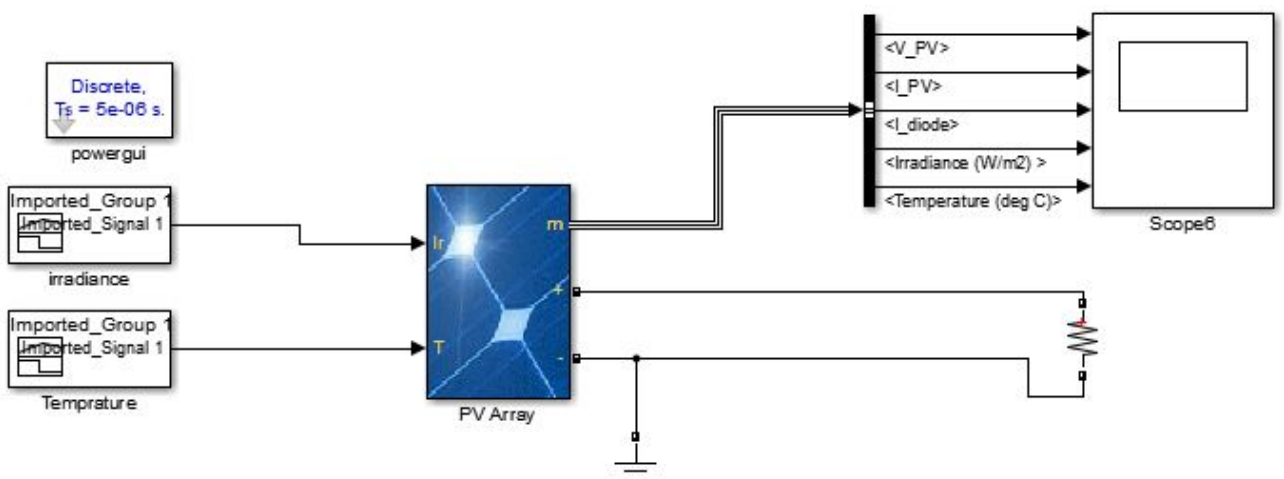


Figure 4.3: PV array MATLAB model[source:Author of thesis]

4.3.1 Effect of Solar radiation variation on PV model

The performance of the PV array depends on the solar radiation of the selected site. In order to determine the effect on solar radiation on the PV array performance simulations are

performed by varying solar radiation and keeping the temperature constant and the result is given in the following figure.

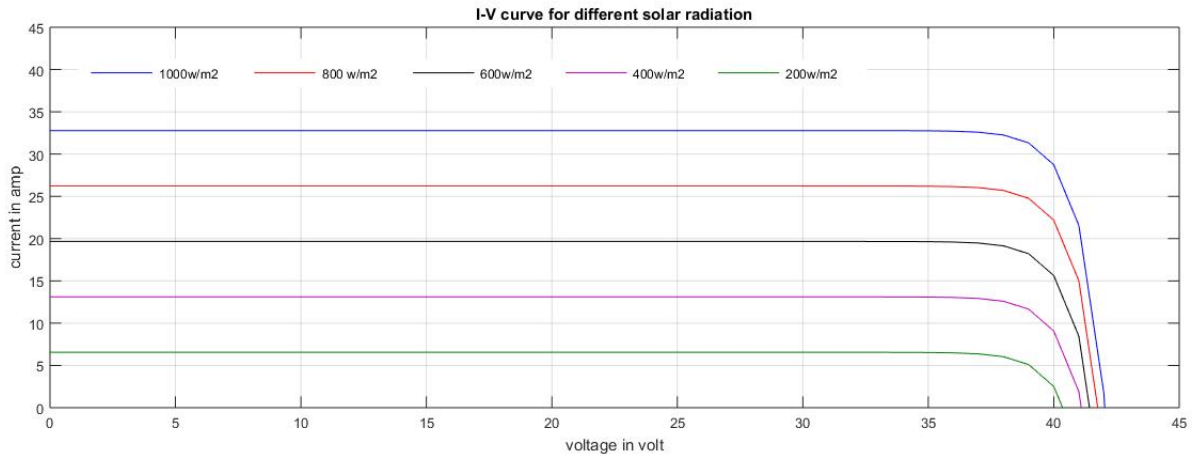


Figure 4.4: I-V curve for different solar radiation [source:Author of thesis]

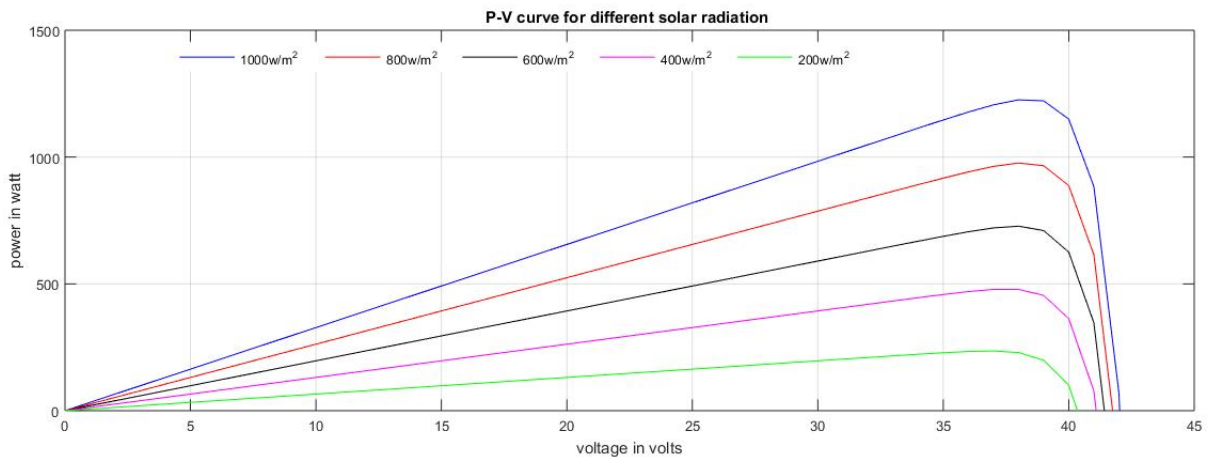


Figure 4.5: P-V curve for different solar radiation [source:Author of thesis]

As it can be seen from Fig4.4, the PV cell current is strongly dependent on the solar radiation. However, the voltage is staying almost constant and it is not varying much. It is very clear that current generated increases with increasing solar irradiance and maximum output power also increases.

4.3.2 Effect of Temperature variation on PV model

from the simulation result it is shown that for a given solar radiation, when the cell temperature increases the open circuit voltage drops and the Powers of the PV module decreases as shown in figure 4.6 and figure 4.7 respectively.

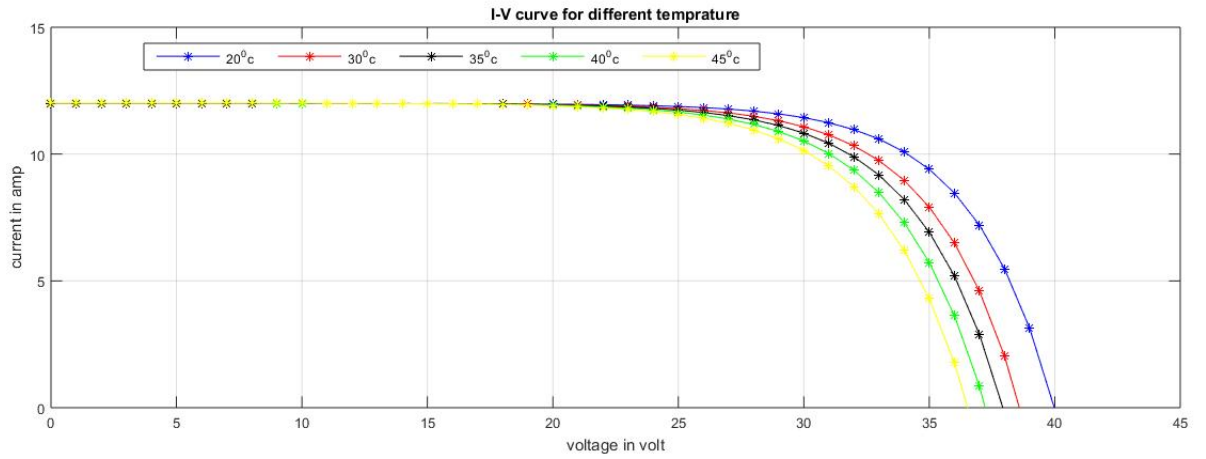


Figure 4.6: I-V curve for different cell Temperature [source:Author of thesis]

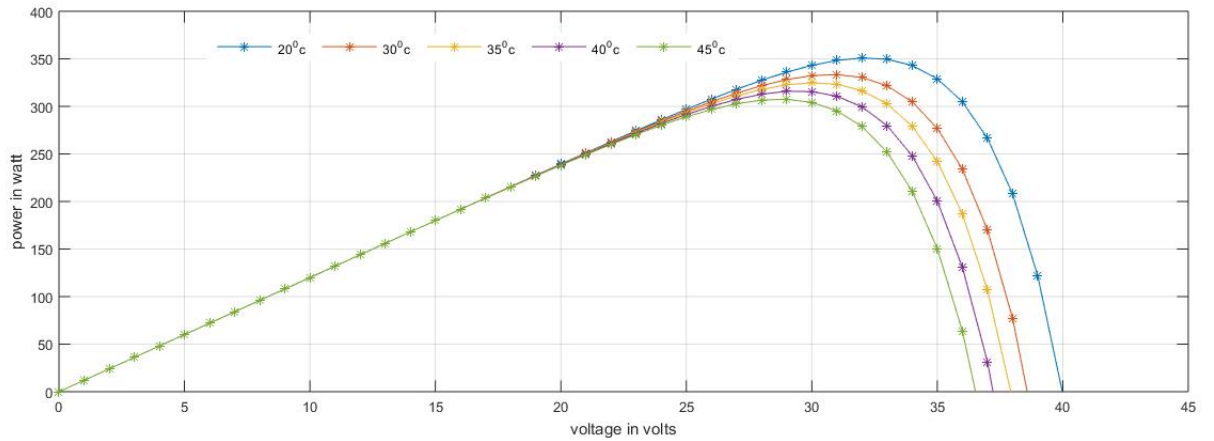


Figure 4.7: P-V curve for different cell Temperature [source:Author of thesis]

4.3.3 Simulation result of PV array

The PV array has two inputs. These are radiation in $KWH/m^2/day$ and temperature in degree kelvin (0k). The average solar radiation of the selected site is $5.38 KWH/m^2/day$ and the average temperature of the site is 296.7^0k . The MATLAB generated for both signal is given in figure4.8 and figure4.9 below.

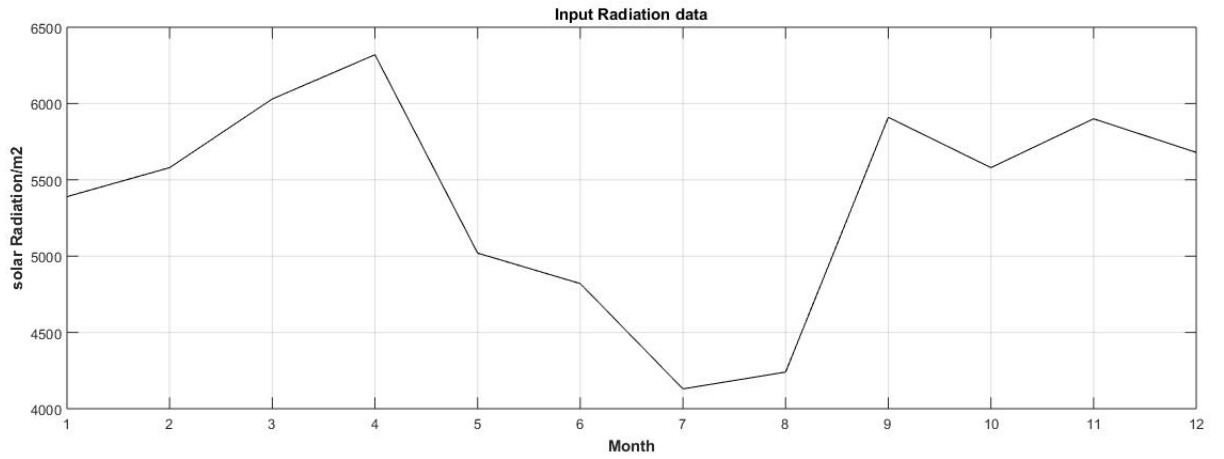


Figure 4.8: input radiation data [source:Author of thesis]

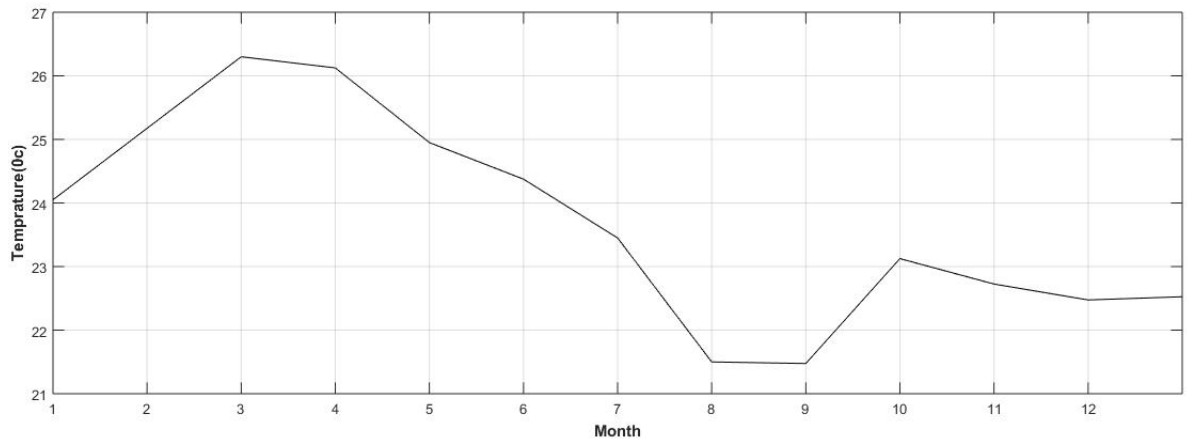


Figure 4.9: input temperature data [source:Author of thesis]

After performing simulation the PV array output voltage is given in the figure4.10.

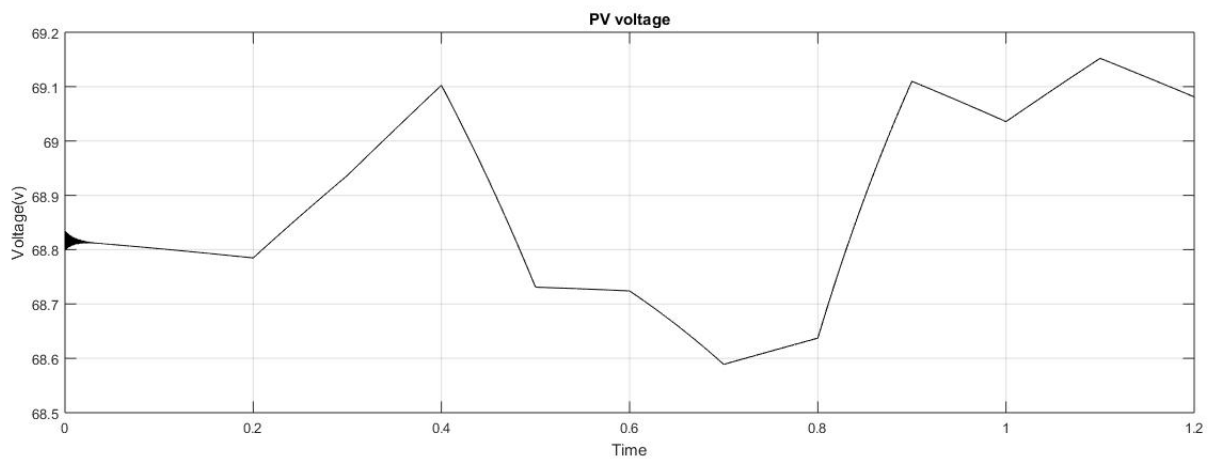


Figure 4.10: Matlab simulation Result of PV voltage [source:Author of thesis]

4.3.4 DC-DC converter

The DC/DC converters are widely used in regulated switch mode DC power supplies. By a PV array an unregulated DC voltage is fed to converter and therefore it will be fluctuating due to changes in radiation and temperature. In these converters the average DC output voltage must be controlled to be equated to the desired value although the input voltage is changing. In recent years, dc-dc converters are widely used in switched mode power supplies. These converters are generally used either to step down (Buck) or step up (Boost) an unregulated dc input voltage. There are various dc-dc converter topologies such as buck, boost, buck-boost, Cuk and full bridge converter. Of these five converters, only the buck and boost are basic converter topologies. The other converters are derived from these two basic converter topologies. Each converter topology has its own principle of operation, advantages and disadvantages [48]. **Design of DC-DC Boost converter :-** DC-DC converter is called Boost converter when average output voltage is higher than input voltage. A boost converter is used in renewable energy systems to step up unregulated dc input voltage to a higher constant output voltage that is required by loads and batteries. The design and development of boost converter is mainly concerned with its efficiency, output power and ease of design. Renewable energy such as solar and wind uses dc-dc boost converter as a medium of power transmission to perform the process of energy absorption and injection to loads and batteries. This process of energy absorption and injection is performed by a combination of four components which are diode, inductor, output capacitor and electronic switch. The connection of boost converter is shown in figure4.11 [49]. This process of energy absorption and injection will constitute of switching cycle. In other words the average output voltage is controlled by switches on and off duration. At constant switching frequency, adjusting the on and off duration of switch is called pulse width modulation switching (PWM). The switching duty cycle, D is defined as the ratio of the on duration to the switching time period. The energy absorption and injection with the relative length of switching period will operate the converter in two different modes known as continuous conduction mode (CCM) and discontinuous conduction mode [48] [49].

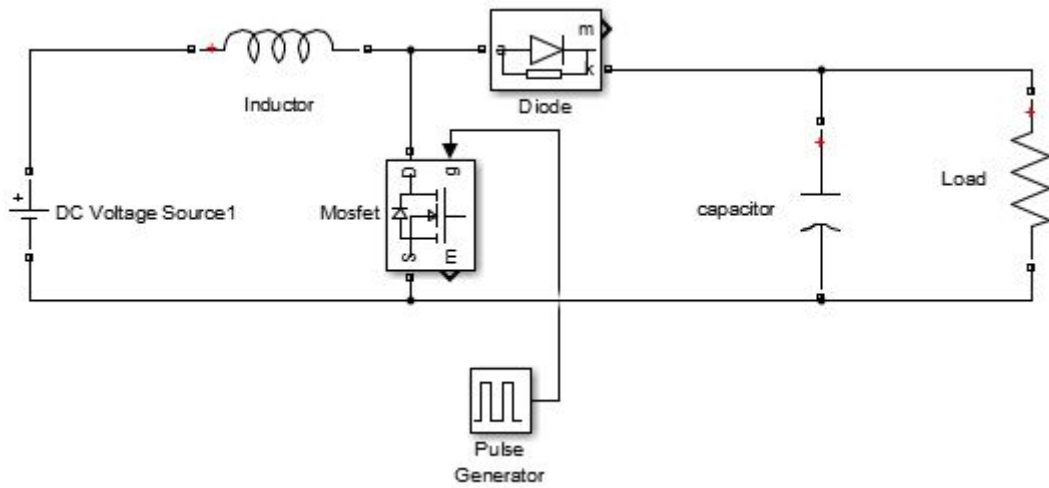


Figure 4.11: Equivalent circuit of DC-DC Boost converter [48]

The continuous conduction mode is divided into two modes. Mode 1 begins when switch SW is turned on at $t=t_{on}$ as shown in figure 4.12. The input current rises and flows through inductor L and switch SW. In Mode 1 energy is stored in the inductor.

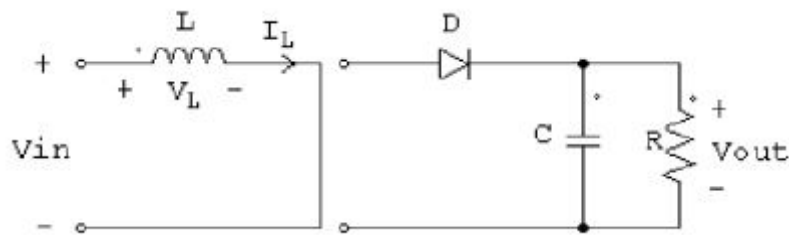


Figure 4.12: Mode 1- Equivalent circuit of boost converter during t_{on} [49]

Mode 2 begins when the switch is turned off at $t=t_{off}$. That current which was flowing through the switch will now flow through L , D , C , and load R as shown in figure 4.13.

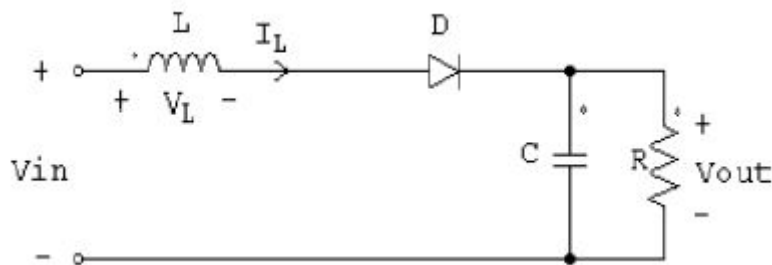


Figure 4.13: Mode 2- Equivalent circuit of boost converter during t_{off} [49]

The inductor current falls until the switch is turned on again in next cycle. The energy transferred to the load will be that energy which was stored in the inductor. Hence, the

output voltage obtained will be more as compared to the input voltage and is expressed as:

$$V_{out} = \frac{V_{in}}{1 - D} \quad (4.14)$$

Where, V_{out} denote output voltage, D denotes Duty cycle and V_{in} is the input voltage [48] [49]. In order to operate the converter in continuous conduction mode, the value of inductance is calculated such that the inductor current I_L flows continuously and never falls to zero. Thus, L is given by

$$L_{min} = \frac{(1 - D)^2 DR}{2f} \quad (4.15)$$

Here, L_{min} denotes the minimum inductance, D the duty cycle, R the output resistance and f is the switching frequency of the switch.

For the desired output voltage ripple the required output capacitance is given by

$$C_{min} = \frac{D}{RfV_r} \quad (4.16)$$

Where C_{min} denotes the minimum capacitance, D is duty cycle, R represents output resistance, f the switching frequency of switch SW and V_r is output voltage ripple factor [?]. V_r can be expressed as

$$V_r = \frac{\Delta V_{out}}{V_{out}} \quad (4.17)$$

In this paper, a boost converter operated in continuous conduction mode is designed to step up an input voltage of 68V to a higher output voltage of 220V. The simulation result of the boost converter is given below.

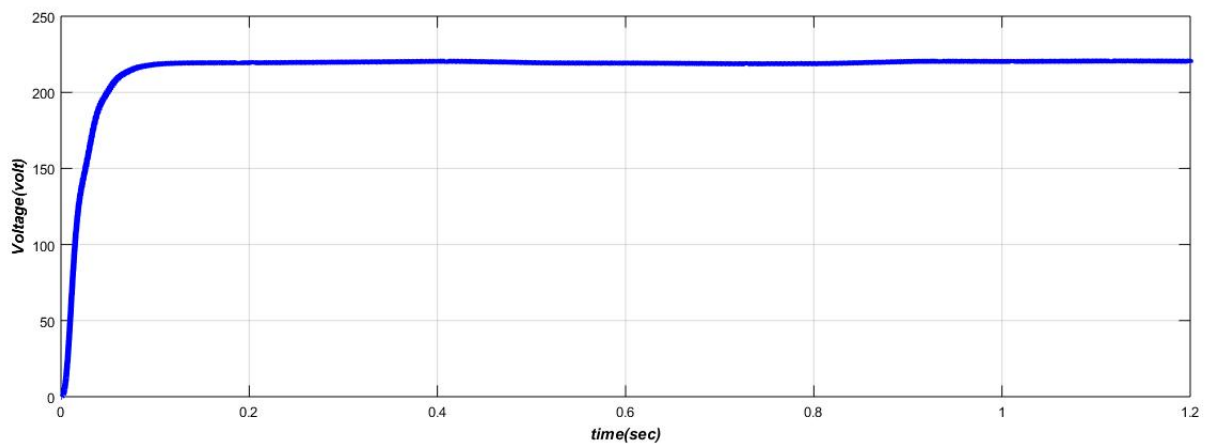


Figure 4.14: Simulated response of output voltage of Boost converter [source:Author of thesis]

4.3.5 Design and modeling of three phase inverter

The main aim of these design is to provide three phase voltage source to the load. **Sinusoidal PWM :-** SPWM is very popular and easy to implement using comparators. The SPWM Simulink system model is built in Figure 4.15 . It has the following blocks: (1) Sinusoidal wave generators, (2) High-frequency triangular wave generator, and (3) comparators.

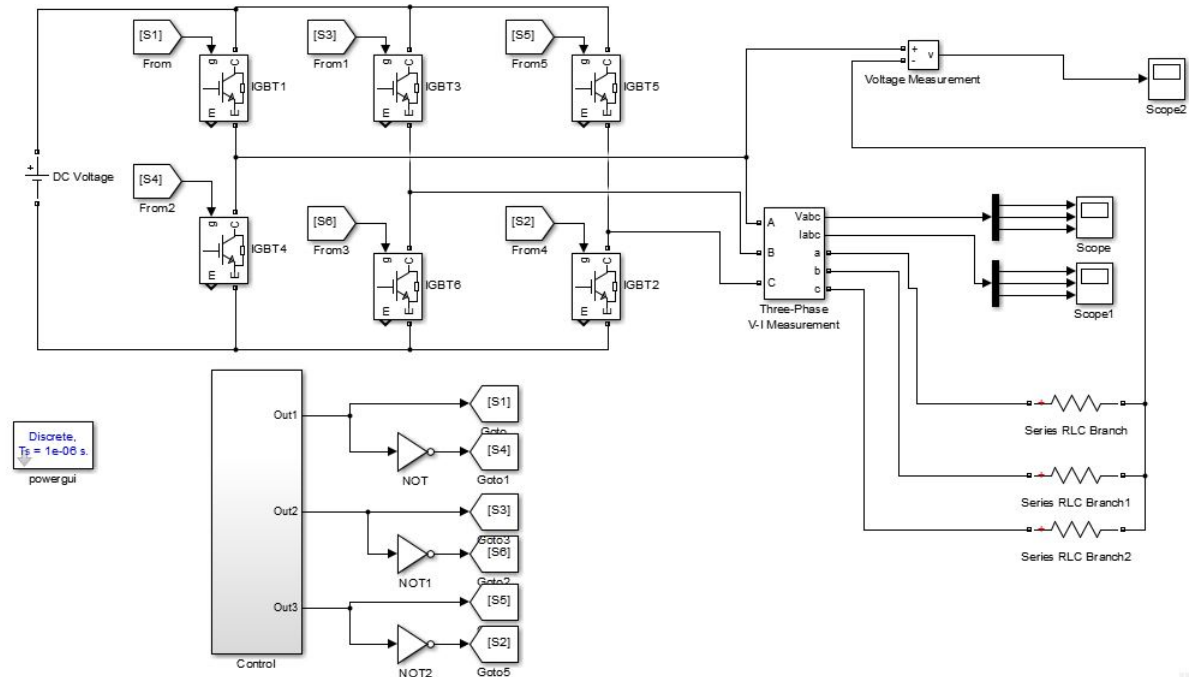


Figure 4.15: SPWM System Model [49]

A three-phase voltage set (V_{ref} , V_{bref} , and V_{cref}) of fixed amplitude is compared in three separate comparators with a common triangular carrier waveform of fixed amplitude as shown in the same figure. The output of the comparators form the control signals for the three legs of the inverter composed of the switch pairs (S1; S4), (S3; S6), and (S5; S2), respectively. From these switching signals and the DC bus voltage, PWM phase-to-neutral voltages (V_{an} , V_{bn} , and V_{cn}) are obtained. In the Simulink model, the simulation is performed under the following conditions:

$$V_{dc} = 220V, \text{ switching frequency} = 15KHz, \text{ Inverter frequency} = 50Hz$$

4.3.6 Storage Battery Designing and sizing

In any off grid or standalone renewable hybrid system the battery bank is undoubtedly the most important component. The power generated by the renewable sources will become totally meaningless if there is no storing device to store those generated power safely and efficiently. As the power generated by the renewable sources is unpredictable in nature, so there may be shortage of generated power sometimes. At that instant some back power will

be needed. During that time the batteries will provide that power to meet the demand. On the other hand when surplus power will be produced by the sources, the batteries will store that excess power by charging themselves. In case of hybrid power system, there is an urgency to connect more than one battery, to form a battery bank.

Battery banks which are generally used in hybrid power systems are of Lead acid type. But the best kinds of batteries to use in renewable hybrid system are deep-discharge lead-acid batteries, which are spatially designed for the specified purpose. The batteries used in hybrid power systems operate under different specified conditions and it is very tough to predict when energy will be extracted from the batteries or supplied to the batteries.

Battery size :-

$$BatteryCapacity = L * C_n = 888.7Ah * 4 = 3554.8Ah \quad (4.18)$$

Where, Cn= 5

$$Numberofbattery = \frac{3554.8Ah}{200Ah} = 17.774 = 18 \quad (4.19)$$

$$Batteryinstring = \frac{Busvoltage}{batteryvoltage} = \frac{220}{12} = 18 \quad (4.20)$$

$$BatteriesinParallel = \frac{numberofbattery}{batteryinstring} = \frac{18}{18} = 1 \quad (4.21)$$

The Battery model provided in matlab sim power systems is Used for this thesis as shown in figure4.16

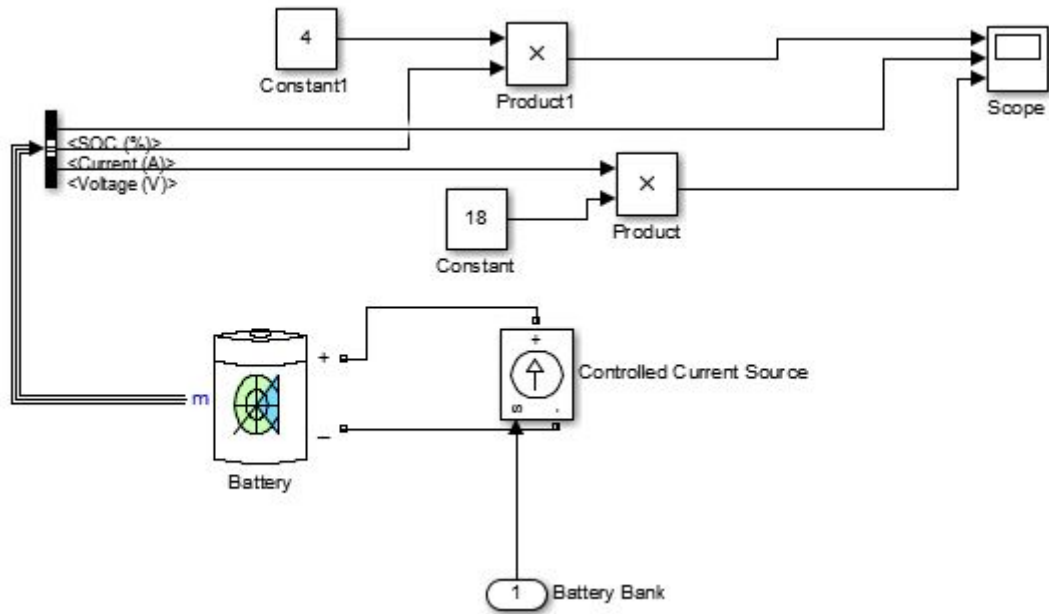


Figure 4.16: Battery Model [source:Author of thesis]

This battery block implements a generic model parameterized to represent most popular types of rechargeable batteries.

4.4 Modeling and Design of Biomass system

4.4.1 Biomass Gasification parameters

Coffee husk has a high calorific value and a low ash content. Hence it can be used to generate electricity through biomass gasification with easy ash disposing ways. The high calorific value low ash content and easily accessibility make coffee husk an ideal row material for generating in rural areas. It is also feasible and helps protecting the environment and produces sustainable energy. Gasification parameters, which are the basic and relevant parameters regarding biomass gasification, operation and performance. **A. Gas flow rate :-** The gasifiers required power output (KW), is an important parameter in which the designer makes a preliminary estimation of the amount of fuels to be feed to the gasifier and the amount of gasifying medium. The volume flow rate of the product gas, V_g (Nm^3/s), from its desired lower heating value, LHV_g (MJ/Nm^3), is found to be net lower heating value can be calculated from its composition.

$$V_g = \frac{P}{\text{LHV}} \quad (4.22)$$

B. Fuel feed rate :- To find the biomass feed rate, m_f , the required power output is divided by the lower heating value of the biomass (LHV_g) and by the gasifier efficiency, η .

$$M_f = \frac{P}{\eta * LHV} \quad (4.23)$$

C. Flow rate of gasifying medium :- The amount of gasification medium has a major influence on yield and composition of the product gas. For an air-blown gasifier, the amount of air required, M_a , for gasification of unit mass of biomass is found by multiplying it by an Equivalence ratio.

$$M_a = M_{th} * E_R \quad (4.24)$$

Where, E_R is the equivalence ratio. For a fuel feed rate of M_f , the air requirement of the gasifier M_{fa} is

$$M_{fa} = M_{th} * E_R * M_f \quad (4.25)$$

OR

$$M_{fa} = V_g * \rho_g \quad (4.26)$$

Here, ρ_g is the density of the medium at the gasifiers operating temperature and pressure. For a biomass gasifier 0.25 may be taken as the first guess for the equivalence ratio.

D. Equivalence ratio (ER) :- It is the ratio of the actual air-fuel ratio to the Stoichiometric air-fuel ratio. This term is generally used for air deficiency situations, such as those found in a gasifier.

$$E_R = \frac{Actual A/F}{Stoichiometric A/F} \quad (4.27)$$

E. Fluidization Velocity :- The range of Fluidizing velocity, V_g , in a babbling bed depends on the mean particle size of the bed materials. The range should be within the minimum fluidization and thermal velocity of the mean bed particles. The particle size may be with in group B or Group D of Geldart's powder classification.

F. Cross sectional Area :- The inside cross-sectional area of the Fluidized bed gasifier, A_b , is found by dividing the volumetric flow rate of the product gas V_g by the chosen superficial gas or Fluidization velocity through it, U_g , the operation temperature and pressure.

$$A_b = \frac{V}{U} \quad (4.28)$$

The Volume of air at the operating temperature and pressure, V_g , is estimated from the mass of air (or other medium), M_{fa} , required for gasification as well as for fluidization. Thus, V_g , is necessarily the gas passing through the grate and the bed.

4.4.2 Gasifier Height

1. Fluidized Bed height :- the bed height (or depth) of a bubbling fluidized bed gasifier is an important design bed parameter. Gas-solid gasification reaction are slower than combustion reactions. So, a bubbling bed gasifier is necessarily deeper than a bubbling bed combustor, which is typically 1 to 1.5 meter deep for units larger than 1m in diameter.

2. free board height :- the empty space above the bed , the freeboard allows entrained particles to drop back in to it. A bubbling turbulence bed must have such a free board section to help avoid excessive loss of bed material through entrainment and to provide room for conversion of finer char particles.

4.4.3 Gas Production rate

The gas flow rate (m^3/s) can be calculated from the primary air flow if the nitrogen content in the producer gas is known. The gas flow rate can be measured by orifice plates, ventures, pitot tubes or rota meters placed in the gas flow (knoef etal 2005). Specific gas production rate is the volumetric flow rate of gas per unit area based on the reactor diameter. The gas volume is measured at normal condition (1atm, 0^0c).

$$Gasproductionrate = \frac{Airflowrate^{\frac{3.76}{4.76}}}{Nitrogenmolefractionofdryproducergas} \quad (4.29)$$

The power output from the gasification process based on each individual agricultural feed stoke is then obtained as

$$Poweroutput(KW) = GasflowRate * LHV \quad (4.30)$$

4.4.4 Biomass system Designing and sizing

From the total 43KW power demand of the village, Biomass has covered 83% of the load demand which is equal to 35.5KW. The electrical power generating capacity of the available coffee husk in Gumay woreda is estimated by the following formula.

$$Inputpower = \frac{Outputpower}{Efficiency} \quad (4.31)$$

Assume the overall conversion efficiency of Gassification is 25% [50].

$$InputPower = \frac{35500W}{0.25} = 142,000W = 0.142MW \quad (4.32)$$

Coffee husk has a lower heating value of $17.2 \frac{MJ}{Kg}$ [51]. Therefore the Biomass required for an hour to generate the input power is found to be

$$BiomassInput(Kg/hr) = 0.142MW * \frac{Kg}{17.2MJ} * \frac{1MJ}{1MW - s} * \frac{3600s}{hr} = 29.7 \frac{Kg}{hr} \quad (4.33)$$

Further it is assumed that the Dual fuel generator works 20 hours per day and 365 days per year. Therefore, the Biomass required per year is calculated as follows

$$Biomassinput(Kg/year) = 29.7 \frac{Kg}{hr} * 20 \frac{hr}{day} * 365 \frac{days}{year} = 216,962.79 \frac{Kg}{year} \quad (4.34)$$

If we assume, 10% of coffee husk produced is wasted and 30% of coffee husk produced is useful for compost and other application then the remaining 60% is used for supping power to the village.

4.5 Modeling of Fuzzy controller for the hybrid system

4.5.1 Fuzzy controller design

Fuzzy logic control appears very useful when linearity and time invariance of the controlled process cannot be assumed, when the process lacks a well posed mathematical model, or when human understanding of the process is very different from its model [52]. Fuzzy logic control provides a formal methodology for representing, manipulating and implementing a humans experience based knowledge about how to control a system. Fuzzy logic uses human knowledge and expertise to deal with uncertainties in the process of control. Fuzzy controller block diagram is shown in Figure 4.17. It has four main parts: (i) Fuzzification interface, simply modifies and converts inputs into suitable linguistic values so that can be compared to the rules in the rule base. (ii) Rule base, holds the knowledge in the form of a set of rules, of how best to control the system. The collection of rules is called a rule base. The rules are in If Then format and formally the If side is called the conditions and the Then side is called the conclusion. The computer is able to execute the rules and compute a control signal depending on the measured inputs error (e) and change in error (dE). In a rule based controller the control strategy is stored in a more or less natural language. A rule base controller is easy to understand and easy to maintain for a non- specialist end

user and an equivalent controller could be implemented using conventional techniques. (iii) Inference mechanism, evaluates which control rules are relevant at current time and then decides what the input to the plant should be. (iv) Defuzzification is when all the actions that have been activated are combined and converted into a single non-fuzzy output signal which is the control signal of the system. The output levels are depending on the rules that the systems have and the positions depending on the non-linearities existing to the systems. To achieve the result, develop the control curve of the system representing the I/O relation of the systems and based on the information; define the output degree of the membership function with the aim to minimize the effect of the non-linearity interface, converts the conclusions reached by the inference mechanism into crisp ones. The affectivity of the fuzzy models representing nonlinear input-output relationships depends on the fuzzy partition of the input output spaces. Therefore, the tuning of membership functions becomes an important issue in fuzzy modeling.

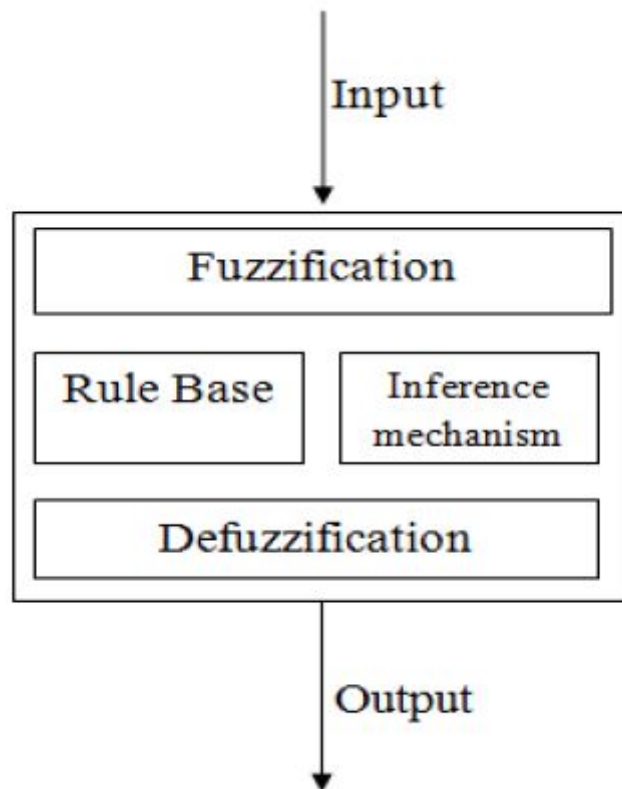


Figure 4.17: Block Diagram of fuzzy logic controller[source:Author of thesis]

In this thesis, A fuzzy logic controller (FLC) is designed to adjust and modify the output continuously based upon the input power from the solar, Biomass and Battery The steps to design fuzzy logic control system are: (1) Choosing the fuzzy controller inputs and outputs (2) Partition the universe of discourse or the interval spanned by each variable into a number

of fuzzy subsets, assigning each a linguistic label (3) Assign or determine a membership function for each fuzzy subset (4) Assign the fuzzy relationships between the inputs or states fuzzy subsets on the one hand and the outputs fuzzy subsets on the other hand, thus forming the rule-base (5) Fuzzify the inputs to the controller (6) Use fuzzy approximate reasoning to infer the output contributed from each rule (7) Aggregate the fuzzy outputs recommended by each rule (8) Apply defuzzification to form a crisp output

a) fuzzifier Design

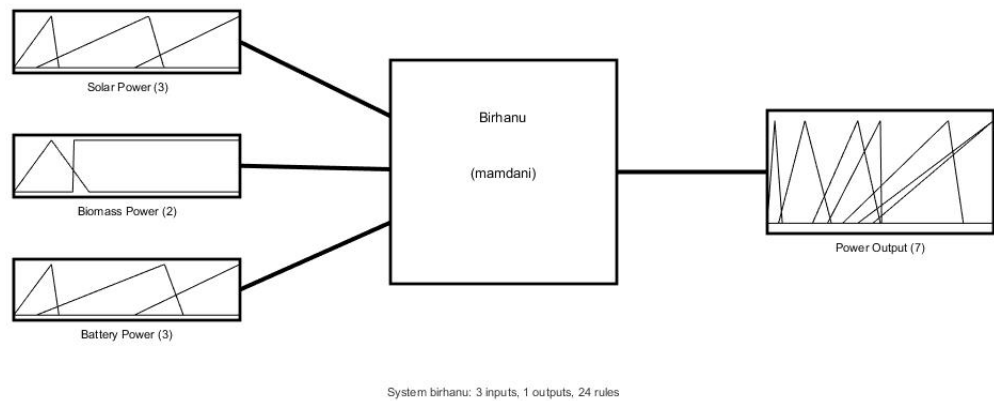


Figure 4.18: Fuzzy control model[source:Author of thesis]

Power from the solar, Battery and Biomass are the inputs to the fuzzy logic controller and the output power is the output of the fuzzy logic controller. The input signal gives the measure of the power level. Based on the input signal the output is sent. The solar power input has three triangular membership functions. These are small, medium and large. The membership function of the solar power input and the parameter ranges of the three membership functions are given in figure 4.19 and table4.3.

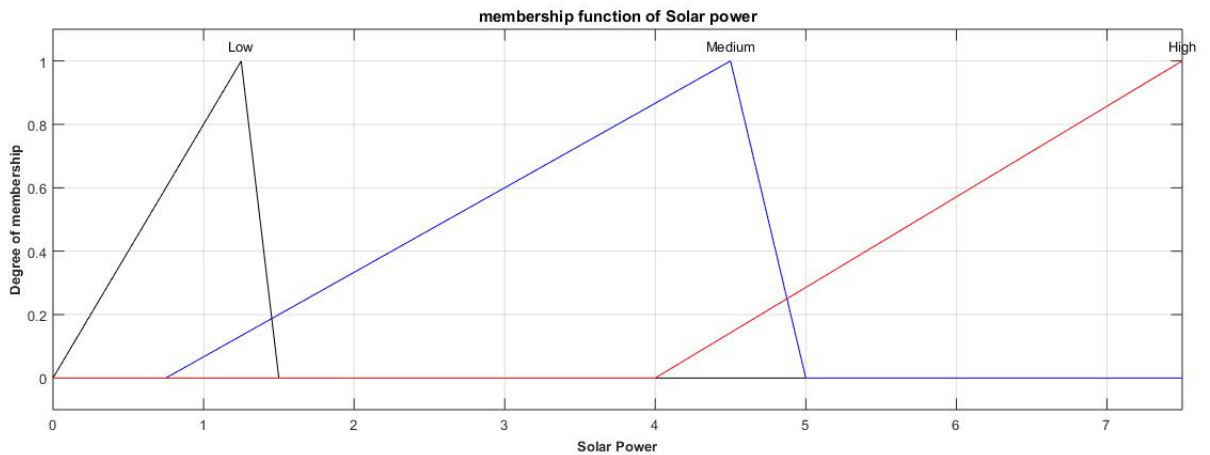


Figure 4.19: Membership function for Solar Power[source:Author of thesis]

Table 4.2: Linguistic variable and parameter range for the solar power input

Name	Type	Parameter Range
Small	Triangular	[0 1.25 2.5]
Medium	Triangular	[2 3.25 5]
Large	Triangular	[4 7.5 7.5]

The biomass power input has two trapezoid membership function which are expressed by the linguistic variable nonfunctional and functional. The membership function of the solar power input and the parameter ranges of the three membership functions are given in figure 4.19 and table4.3.

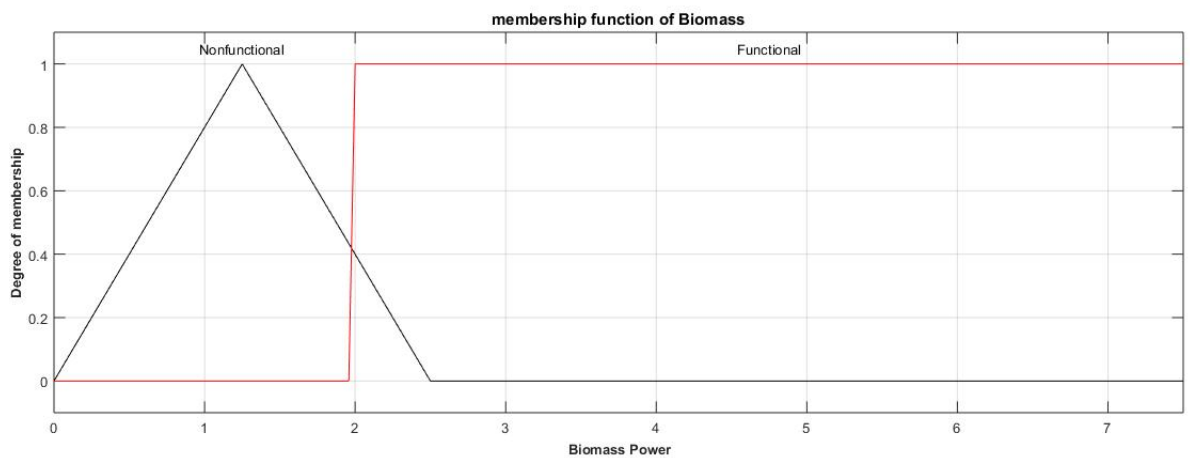


Figure 4.20: Membership function for Biomass Power[source:Author of thesis]

Table 4.3: Linguistic variable and parameter range for the Biomass power input

Name	Type	Parameter Range
Non-functional	Trapezoid	[0 0 2 2.5]
functional	Trapezoid	[1.5 2 7.5 7.5]

The battery power input has three triangular membership function which are expressed by the linguistic variable small, medium and large. The membership function of the battery power input and the parameter ranges of the three membership functions are given in figure 4.21 and table4.4.

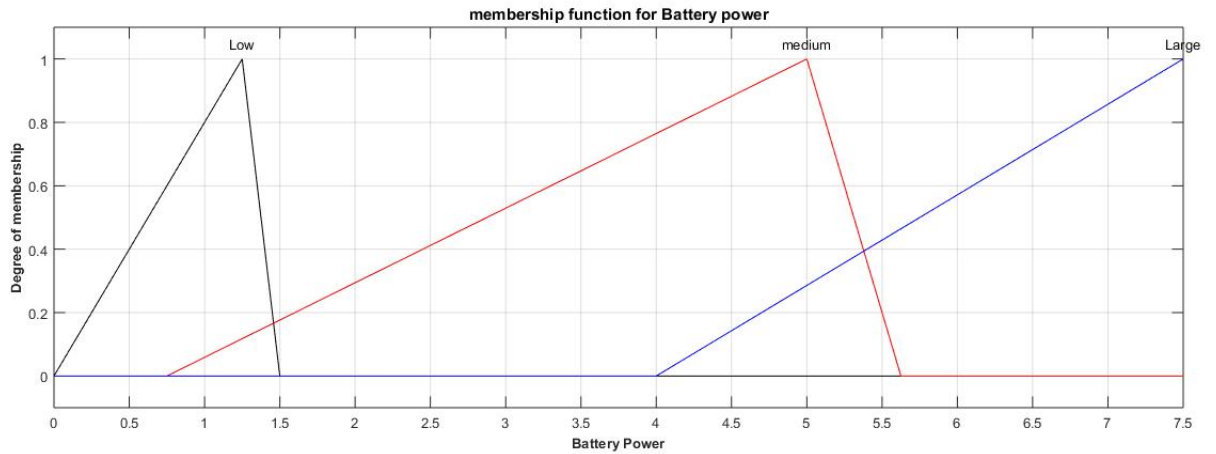


Figure 4.21: Membership function for Battery Power[source:Author of thesis]

Table 4.4: Linguistic variable and parameter range for the battery power input

Name	Type	Parameter Range
Small	Triangular	[0 2.5 3]
Medium	Triangular	[2 3.25 5]
Large	Triangular	[4 7.5 7.5]

The battery power input has three triangular membership function which are expressed by the linguistic variable small, medium and large. The membership function of the battery power input and the parameter ranges of the three membership functions are given in figure 4.21 and table4.4.

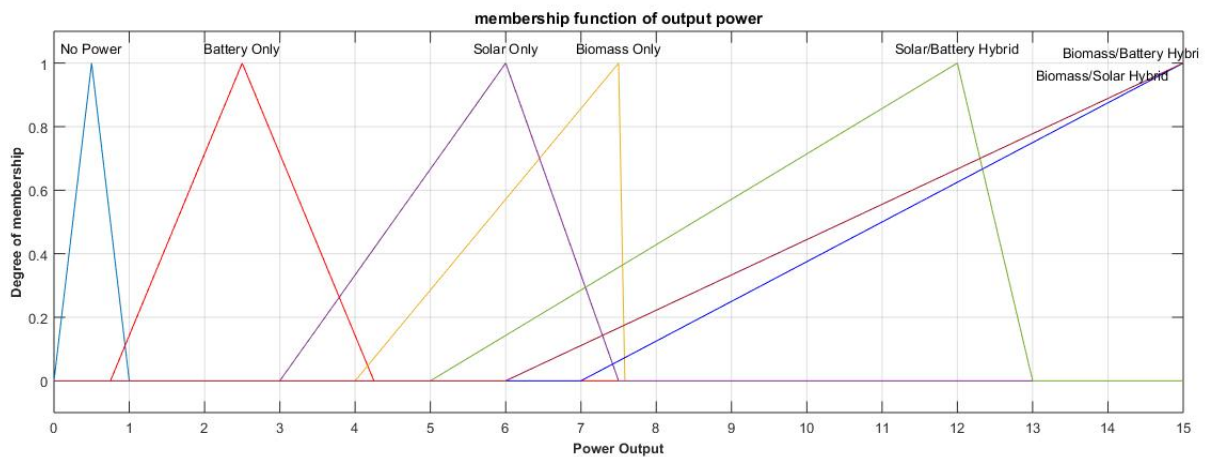


Figure 4.22: Membership function for output Power[source:Author of thesis]

4.6 Modeling of Fuzzy Logic control rules

Based on the descriptions of the input and output variables defined with the FIS Editor, the Rule Editor allows you to construct the rule statements automatically, by clicking on

and selecting one item in each input variable box, one item in each output box, and one connection item. Choosing none as one of the variable qualities will exclude that variable from a given rule. Figure 4.23 shows the fuzzy logic rules and operation of the system in different operating conditions.

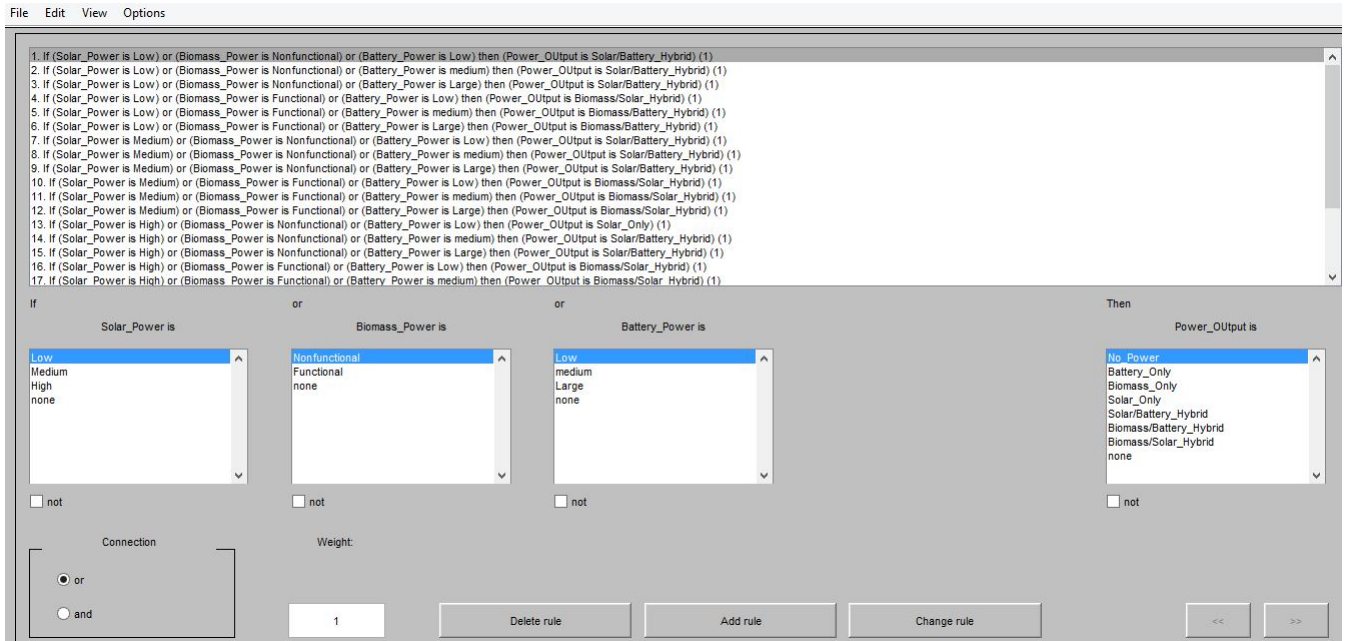


Figure 4.23: Fuzzy Logic Rules[source:Author of thesis]

4.7 Overall Fuzzy Logic Control System

The overall fuzzy logic system consists of the PV system, the Battery and the Dual fuel System for Biomass power generation. Each system is separately modeled and simulated and they become the input to the Fuzzy logic controller. Based on the available resource, the rule selects one or more of the inputs to supply power to the load.

Hence in figure 4.24, solar power indicate the output from solar energy, biomass power indicates electric energy from the biomass resource and battery power indicates power from battery Bank. The multiport conditional switch will take an action according to the rules written in fuzzy logic control.

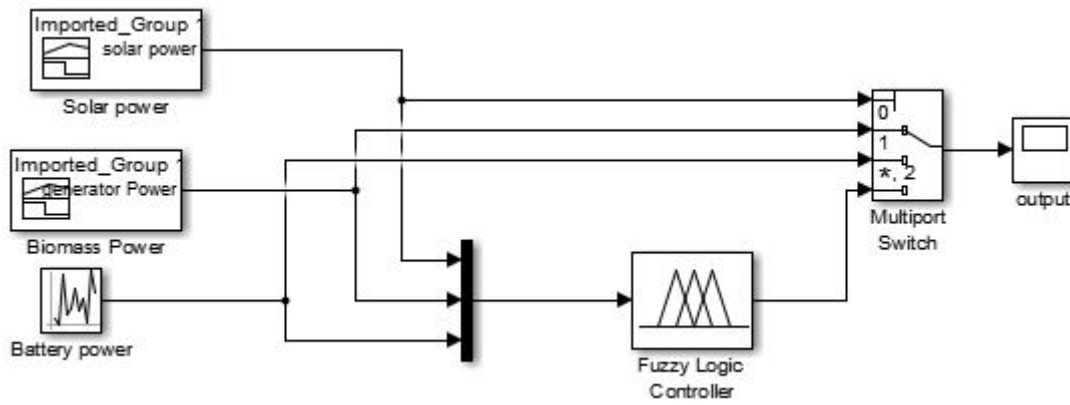


Figure 4.24: Overall Fuzzy logic Control System[source:Author of thesis]

4.8 Matlab Simulation Result of Fuzzy Logic Control

As the simulation result depends on the availability of different renewable energy resource, rules are constructed using graphical Rule Editor Interface. Based on the descriptions of the input and output variables defined with the FIS Editor, the fuzzy logic controller selects the best resource which are subject to supply the intended power demand and the result is shown in figure4.25.

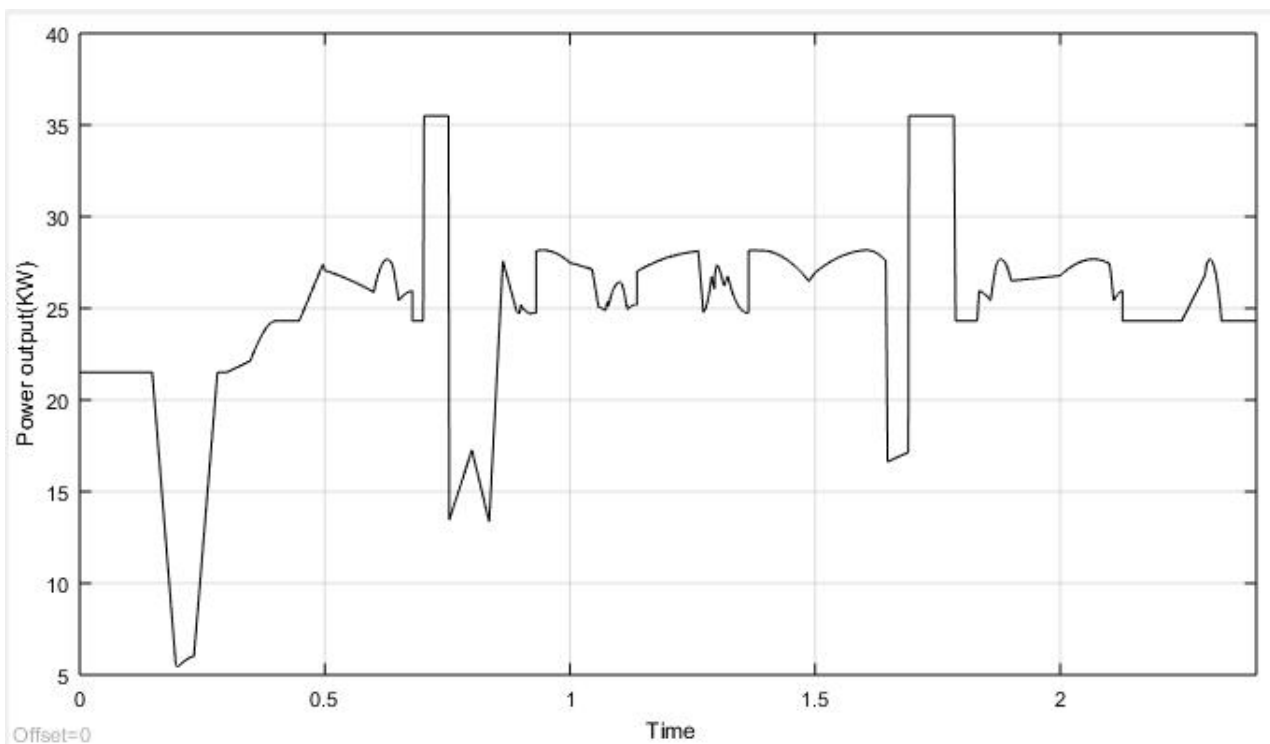


Figure 4.25: Simulation result when all energy forms are available[source:Author of thesis]

The simulation result shows that based on the written rule, the fuzzy logic controller selects the best hybrid combination of the available resource or a single energy source to supply the intended power demand.

4.9 Cost Estimation of the system

4.9.1 Cost Evaluation of Solar PV Power Generation

The electrical Demands considered for the selected villages are lighting, radio, television, refrigerator and water pumping and for lighting purpose, energy saving lamps of compact fluorescent type are recommended. The costs are estimated according to the current local and global price of the components. The cost of this system includes acquisition (purchasing) costs, operating costs, maintenance costs, and replacement costs.

4.9.2 Investment Cost PV and Battery

Investment costs include the cost purchasing PV modules, batteries, Diesel fuel generator, inverter, converter, management unit, cables, and other accessories used in the installation including labors. The average cost of the PV is \$1/Wp and the total power of the PV system is 7500W.

Table 4.5: The used cost data

Item	PV	Battery	Installation	O&M/Year
Cost	\$1/Wp	\$314.8/Piece	10% of system cost	2% of system cost

4.9.3 Life cycle cost(LCC) of PV system

The LCC of the PV system includes the sum of all the present worth (PWs) of the costs of the PV modules, storage batteries, inverter, the cost of the installation, and the maintenance and operation cost (M& O) of the system. The LCC of an item consists of the total costs of owning and operating an item over its lifetime, expressed in today's money. The costs of a stand-alone PV system include acquisition costs, operating costs, maintenance costs, and replacement costs. All these costs have the following specifications [53] The initial cost of the system (the capital cost) is high. There are no fuel costs. Maintenance costs are low. The lifetime N of all the items is considered to be 20 years, except that of the battery which is considered to be 10 years. Thus, an extra 1 groups of batteries (18 batteries) have to be purchased, after 10 years. Assuming an inflation rate i of 7.26% [54] and a discount or interest rate d of 5.07% [55]. Therefore, the PWs of all the items can be calculated and given as follows in table 4.6

Table 4.6: System cost of PV with its accessory

No.	Description	Quantity	Unit Price(\$)	Total Price(\$)
1	Module(200Wp)(CPV)	7500w	\$1.00	7,500.00
2	Battery(200AH)(CB)	18	\$314.80	5,666.40
3	Battery(200AH)(CB1PW)	18		5,964.63
4	DC-AC inverter(CINV)	8000w	\$1,300	1,300.00
5	Operation and maintainance cost(CMPW)			3,751.97
6	Cabling,Switching,holder,plug,divider			1,000.00
7	Installation Cost(CINST)(10% system)			2,518.30
9	LCCPV			27,701.30

As it has shown in table 4.6, the PV array costs(C_{PV}) can be calculated to be \$7,500 and the initial cost of the batteries CB becomes \$5,666.4. The present worth of the extra group of batteries (purchased after $N = 10$ years) CB1PW can be calculated, to be \$5,964.267.

$$CB1PW = CB \left(\frac{1+i}{1+d} \right)^N \quad (4.35)$$

The present worth of the maintenance cost CMPW can be calculated to be \$3751.97, using the maintenance cost per year (M/yr) and the lifetime of the system ($N = 20$ years), from equation 4.40 [?]

$$C_{MPW} = (M/yr) * \left(\frac{1+i}{1+d} \right) * \left[\frac{1 - \left(\frac{1+i}{1+d} \right)^N}{1 - \left(\frac{1+i}{1+d} \right)} \right] \quad (4.36)$$

Therefore, the life cycle cost of the PV system can be calculated by equation 4.37 and is equal to \$27,701.3.

$$LCC_{PV} = CPV + CB + CB1PW + C_{INV} + C_{INST} + CMPW \quad (4.37)$$

The annualized LCC (ALCC) of the PV System can be calculated to be \$1130.5528/year, from [?]

$$ALCC = LCC * \left[\frac{1 - \left(\frac{1+i}{1+d} \right)}{1 - \left(\frac{1+i}{1+d} \right)^N} \right] \quad (4.38)$$

4.9.4 Investment Cost of Biomass Gasifier and Dual Fuel Generator

A power plant should generate a reliable supply of electricity at a possible minimum cost to the investor and consumer. The cost of generation is determined by so many factors principal among them is the investment or capital cost of biomass power projects which is made up of cost of; gasifier, engine generator, civil works, biomass preparation unit,

electricity distribution network and electrical and piping connections to the site of gasifier installation [56].The total investment cost (I) of a biomass energy conversion system is made up of cost of fuel conversion system or gasifier cost (CG), cost of prime mover (CPM), engineering and construction work costs (Cw) and cost of accessories and miscellaneous CA. Thus;

$$I = C_G + C_{PM} + C_w + C_A \quad (4.39)$$

Thus,the total investment cost of a biomass gasification conversion system with all the an-cillaries in table 4.7 estimated by NERC as 3000 \$/kwh [57]

Table 4.7: Biomass Gasification investment cost Breakdown

Item	Capital cost(\$/KW)
Fuel Handling	300
Electrical	250
Converter system(gasifier)	2000
Prime Mover(Engine)	450
Total	3000

As the required power from the required power from the Biomass is 35.5KW the invest-ment cost of the system becomes \$106,500.

Other Economic Parameters used in the cost Analysis of Biomass Power Plant are given in Table

Table 4.8: Economic Parameter for the Biomass Power Plant [57]

Parameter	Value
Investment Cost	3000\$/Kw
Operation and Maintenance Cost	60\$/yr

The maintenance cost of the Biomass system is calculated by using4.40 and it has found to be \$616.962.

$$MC = (M/yr) * \left(\frac{1 + i}{1 + d} \right) * \left[\frac{1 - \left(\frac{1+i}{1+d} \right)^N}{1 - \left(\frac{1+i}{1+d} \right)} \right] \quad (4.40)$$

The life cycle cost of the biomass system becomes \$107,116.962.

$$LCC_{biomass} = I + MC = 106,500 + 616.962 = \$107116.962 \quad (4.41)$$

After cost analysis of biomass and Solar PV system has been done separately the life cycle cost of the system becomes the sum of the life cycle cost of the Solar PV system and the live

cycle of the biomass system. Thus the life cycle cost of the system becomes \$134,817.962.

$$LCC_{system} = LCC_{biomass} + LCC_{PV} = \$107,116.962 + \$27,701 = \$134,817.962 \quad (4.42)$$

The annualized LCC (ALCC) of the system can be calculated to be \$5490.2764/year.

$$ALCC_{system} = LCC * \left[\frac{1 - \left(\frac{1+i}{1+d}\right)}{1 - \left(\frac{1+i}{1+d}\right)^N} \right] \quad (4.43)$$

After the average life cycle cost of the system is determined, the unit electrical cost can be calculated as follows.

$$Unitelectricalcost = \frac{ALCC_{system}}{365 * Loaddemand} = \frac{\$5490.2764}{365 * 245.16} \quad (4.44)$$

$$Unitelectricalcost(\$ / kwh) = \frac{\$5,490.2764}{89,483.4} = \$0.061355 \quad (4.45)$$

CHAPTER 5

CONCLUSION AND RECOMMENDATION

5.1 Conclusion

Electrification of rural areas is very important for sustainable development of our country, Ethiopia. This thesis provides the Design and simulation of an off-Grid Fuzzy Logic Controller Based Hybrid Biomass-Solar PV power generating system for pera Village. The fuzzy logic controller selects the appropriate resource by sensing the type and amount of resource available. Thus the possible power source can be solar energy alone, Biomass energy alone, Battery energy alone, a hybrid of the possible combination of the two or the hybrid of solar, biomass and battery.

As the main objective of this thesis is to Design and simulation of an off-Grid Fuzzy Logic Controller Based Hybrid Biomass-Solar PV power generating system for pera Village, first a renewable energy source assessment has been made. Accordingly, the four year solar sunshine hour data and the ten year biomass resource (coffee husk) data has been collected from national meteorology agency Jimma branch and Gummay woreda coffee quality office respectively. Since the solar resource data available is the solar sunshine hour data, it has been converted in to solar radiation data using Empirical formulas.

After assessment of resource, Load assessment of the village has been made for 200 households, one primary school and one health center. Hence, the total power demand of the village is found to be 43KW. To satisfy this demand 17.4% was covered by solar and the remaining 82.6% was covered by Biomass system.

A PV was sized and as the solar PV power depends on solar radiation and input temperature, simulations were performed to see the impacts of their variation on the performance of the PV. Accordingly, as the input radiation increase the output power of the PV Array increases and as the input temperature increases the output power of the PV decreases. Thus the increase in temperature has a negative impact on PV performance.

Since, the system is a hybrid system a biomass power generating system has also designed that shares the load demand of the village. Accordingly, 35.5KW of power is generated by using coffee husk biomass energy resource. In addition to this a battery bank is designed and sized to supply power when the solar resource is not available. Depending on the resource available fuzzy logic controller is used to select the appropriate power source. The rules which has been written on fuzzy logic controller will consider all the possible cases. Therefore, it is not necessary to simulate a different cases. In addition to the design of the

system cost estimation has been performed using analytical method. Accordingly the total life cycle cost of the system becomes \$134,817.962.

5.2 Recommendation

Government of Ethiopia should grant financial incentives to any power investor interested in investing in renewable energy technologies especially Biomass power plant to encourage its adoption and development in Ethiopia. The future recommendation is the further research could be done to investigate the possibility of using hydro-power whether the data of rivers on Gumay Woreda is collected. If the hydro-power is feasible to use then the composition of Solar/Biomass/Hydro hybrid renewable energy system could be combined in such a way to achieve the best performance of the hybrid system. A further search on different renewable energy would be taken to reach for the unconnected rural households. As the cost analysis has performed using analytical method, it is recommended that further study would be taken for cost optimization using artificial neural network (ANN). Important part of such study is a more deep cost optimization study as well as investigating and updating of prices, investment costs and local conditions. Deep analysis of inverter system and filter design to eliminate the harmonics and improve the efficiency of the inverter is also recommended for future work.

BIBLIOGRAPHY

- [1] J. L. Bernal-Agustn and R. Dufo-Lpez, “Simulation and optimization of stand-alone hybrid renewable energy systems,” *Renewable and Sustainable Energy Reviews*, vol. 13, no. 8, pp. 2111 – 2118, 2009. [Online]. Available: <http://www.sciencedirect.com/science/article/pii/S1364032109000215>
- [2] R. Sharma and S. Goel, “Stand-alone hybrid energy system for sustainable development in rural india,” *Environment, Development and Sustainability*, pp. 1–14, 2013.
- [3] W. bank. (2018, jan) World population. [Online]. Available: <http://www.worldometers.info/world-population/ethiopia-population/>
- [4] W. bank Ethiopia. (2018, jan) Ethiopian energy situation. [Online]. Available: https://energypedia.info/wiki/Ethiopia_Energy_Situation
- [5] K. Kusakana, J. Munda, and A. Jimoh, “Feasibility study of a hybrid pv-micro hydro system for rural electrification,” in *AFRICON 2009*. IEEE, 2009, pp. 1–5.
- [6] L. Africa. (2012, jan) Lighting africa policy report note ethiopia. [Online]. Available: <https://www.lightingafrica.org/publication/lighting-africa-policy-report-note-ethiopia/>
- [7] M. Chegaar, A. Lamri, and A. Chibani, “Estimating global solar radiation using sunshine hours,” *Rev. Energ. Ren*, vol. 1, pp. 7–11, 2008.
- [8] G. Bekele, “Study into the potential and feasibility of a standalone solar-wind hybrid electric energy supply system,” Ph.D. dissertation, KTH, 2009.
- [9] S. G. Deb, “Optimal sizing of a stand-alone solar-wind-battery-dg/biomass hybrid power system to meet the load demand of a typical village at sagar island using genetic algorithm,” Ph.D. dissertation, JADAVPUR UNIVERSITY, 2012.
- [10] J. Ramos-Hernanz, J. Campayo, J. Larranaga, E. Zulueta, O. Barambones, J. Motrico, U. F. Gamiz, and I. Zamora, “Two photovoltaic cell simulation models in matlab/simulink,” *International Journal on Technical and Physical Problems of Engineering (IJTPE)*, vol. 4, no. 1, pp. 45–51, 2012.
- [11] J. Bikaneria, S. P. Joshi, A. Joshi *et al.*, “Modeling and simulation of pv cell using one-diode model,” *International Journal of Scientific and Research Publications*, vol. 3, no. 10, pp. 1–4, 2013.

- [12] G. Venkateswarlu and P. S. Raju, "Simscape model of photovoltaic cell," *Int J Adv Res Electr Electr Instrum Eng*, vol. 2, no. 5, p. 7, 2013.
- [13] D. Bonkougou, Z. Koalaga, and D. Njomo, "Modelling and simulation of photovoltaic module considering single-diode equivalent circuit model in matlab," *International journal of emerging technology and advanced engineering*, vol. 3, no. 3, pp. 493–502, 2013.
- [14] K. S. Deokar and R. Holmukhe, "Analysis of pv/wind/fuel cell hybrid system interconnected with electrical utility grid," *Communication and Power Engineering*, p. 327, 2017.
- [15] R. K. Akikur, R. Saidur, H. W. Ping, and K. R. Ullah, "Comparative study of stand-alone and hybrid solar energy systems suitable for off-grid rural electrification: a review," *Renewable and Sustainable Energy Reviews*, vol. 27, pp. 738–752, 2013.
- [16] A. Rohani, K. Mazlumi, and H. Kord, "Modeling of a hybrid power system for economic analysis and environmental impact in homer," in *2010 18th Iranian Conference on Electrical Engineering*. IEEE, 2010, pp. 819–823.
- [17] É. Piech, "Renewable energy sources," Master's thesis, Akademia Gorniczko-Hutnicza, 2012.
- [18] R. Foster, M. Ghassemi, and A. Cota, *Solar energy: renewable energy and the environment*. CRC Press, 2009.
- [19] K. Janardhan, T. Srivastava, G. Satpathy, and K. Sudhakar, "Hybrid solar pv and biomass system for rural electrification," *Int. J. Chem. Tech. Res. ICGSEE*, vol. 5, no. 2, pp. 802–810, 2013.
- [20] A. Teshale, "Modeling and simulation of fuzzy logic based hybrid power for irrigation system in case of wonji-shoa villages," *Recent Advances on Energy, Environment, Ecosystems, and Development*, pp. 1–16, 2012.
- [21] C. S. Solanki, *Solar photovoltaics: fundamentals, technologies and applications*. PHI Learning Pvt. Ltd., 2015.
- [22] N. Sanke, "Biomass for power and energy generation," *Combustion*, vol. 900, p. 12000C.
- [23] P. Basu, *Biomass gasification, pyrolysis and torrefaction: practical design and theory*. Academic press, 2013.

- [24] R. Gera, H. Rai, Y. Parvej, and H. Soni, “Renewable energy scenario in india: Opportunities and challenges,” *Indian Journal of Electrical and Biomedical Engineering*, vol. 1, no. 1, pp. 10–16, 2013.
- [25] M. M. Hailemariam, T. Mekonnen, and H. Sudheendra, “Novel approach to fuzzy logic controller based hybrid solar/micro hydro/bio-mass generation, a real time analysis (barsoma village, ethiopia.)”
- [26] M. Lubwama, “Technical assessment of the functional and operational performance of a fixed bed biomass gasifier using agricultural residues,” 2009.
- [27] H. Knoef, *Handbook biomass gasification*.
- [28] G. A. Richards and K. H. Casleton, “Gasification technology to produce synthesis gas,” *Synthesis Gas Combustion: Fundamentals and Applications*, p. 403, 2010.
- [29] G. A. Richards, K. H. Casleton, and N. T. Weiland, “Syngas utilization,” *Synthesis Gas Combustion: Fundamentals and Applications, Taylor & Francis*, pp. 193–222, 2010.
- [30] A. Luque and S. Hegedus, *Handbook of photovoltaic science and engineering*. John Wiley & Sons, 2011.
- [31] L. E. Weldemariam, “Genset-solar-wind hybrid power system of off-grid power station for rural applications,” 2010.
- [32] W. Kellogg, M. Nehrir, G. Venkataramanan, and V. Gerez, “Generation unit sizing and cost analysis for stand-alone wind, photovoltaic, and hybrid wind/pv systems,” *IEEE Transactions on energy conversion*, vol. 13, no. 1, pp. 70–75, 1998.
- [33] H. A. Elreesh, “Design of ga-fuzzy controller for magnetic levitation using fpga,” Ph.D. dissertation, The Islamic University of Gaza, 2011.
- [34] J. Yen and R. Langari, *Fuzzy logic: intelligence, control, and information*. Prentice Hall Upper Saddle River, 1999, vol. 1.
- [35] C. W. De Silva, *Intelligent control: fuzzy logic applications*. CRC press, 1995.
- [36] L. A. Zadeh, “Fuzzy logic,” 1988.
- [37] S. R. Wenham, M. A. Green, M. E. Watt, R. Corkish, and A. Sproul, *Applied Photovoltaics*. Routledge, 2013.

- [38] C. A. Gueymard, *The suns total and spectral irradiance for solar energy applications and solar radiation models*. Elsevier, 2004.
- [39] J. Twidell and T. Weir, *Renewable energy resources*. Routledge, 2015.
- [40] M. Iqbal, *An introduction to solar radiation*. Elsevier, 2012.
- [41] J. A. Duffie and W. A. Beckman, "Design of photovoltaic systems," *Solar Engineering of Thermal Processes, Fourth Edition*, pp. 745–773, 2013.
- [42] M. M. Mahmoud and I. H. Ibrik, "Techno-economic feasibility of energy supply of remote villages in palestine by pv-systems, diesel generators and electric grid," *Renewable and Sustainable Energy Reviews*, vol. 10, no. 2, pp. 128–138, 2011.
- [43] B. Tamrat, "Comparative analysis of feasibility of solar pv, wind and micro hydro power generation for rural electrification in the selected sites of ethiopia," Ph.D. dissertation, Addis Ababa University, 2007.
- [44] G. Bekele and G. Tadesse, "Feasibility study of small hydro/pv/wind hybrid system for off-grid rural electrification in ethiopia," *Applied Energy*, vol. 97, pp. 5–15, 2012.
- [45] "Solar Cell structure," <http://www.pveducation.org/pvcdrom/solar-cell-parameters>, 2017, [Online; accessed 19-June-2017].
- [46] L. Castaner and S. Silvestre, *Modelling photovoltaic systems using PSpice*. John Wiley and Sons, 2002.
- [47] T. Ikegami, T. Maezono, F. Nakanishi, Y. Yamagata, and K. Ebihara, "Estimation of equivalent circuit parameters of pv module and its application to optimal operation of pv system," *Solar energy materials and solar cells*, vol. 67, no. 1, pp. 389–395, 2009.
- [48] N. Mohan and T. M. Undeland, *Power electronics: converters, applications, and design*. John Wiley & Sons, 2007.
- [49] S. Masri and P. Chan, "Design and development of a dc-dc boost converter with constant output voltage," in *Intelligent and Advanced Systems (ICIAS), 2010 International Conference on*. IEEE, 2010, pp. 1–4.
- [50] L. P. Bingh, "Opportunities for utilizing waste biomass for energy in uganda," Master's thesis, Institutt for energi-og prosessteknikk, 2010.

- [51] S. Kore, A. Assefa, M. Matthias, and H. Spliethoff, “Steam gasification of coffee husk in bubbling fluidized bed gasifier,” in *Proceedings of the Fourth International Conference on Bioenvironment, Biodiversity and Renewable energies; ISBN*. Citeseer, 2013, pp. 978–1.
- [52] K. M. Passino, S. Yurkovich, and M. Reinfrank, *Fuzzy control*. Addison-wesley Reading, MA, 1998, vol. 20.
- [53] T. Markvart, *Solar electricity*. John Wiley & Sons, 2000, vol. 6.
- [54] Statista. (2017, nov) Ethiopia: Inflation rate from 2010 to 2020 (compared to the previous year). [Online]. Available: <https://www.statista.com/statistics/455089/inflation-rate-in-ethiopia/>
- [55] T. Economics. (2017, nov) Ethiopia interest rate. [Online]. Available: <https://tradingeconomics.com/ethiopia/interest-rate>
- [56] C. Diyoke, S. Idogwu, and U. Ngwaka, “An economic assessment of biomass gasification for rural electrification in nigeria,” *Int. J. Renewable Energy Technol. Res.*, vol. 3, no. 1, pp. 1–17, 2014.
- [57] O. Ohijeagbon and O. O. Ajayi, “Solar regime and lvoe of pv embedded generation systems in nigeria,” *Renewable Energy*, vol. 78, pp. 226–235, 2015.

Appendix A: Matlab Program**A1: for simulation of PV with varying radiation**

```
T = 20+273;
Tref = 25;
Trefk = Tref+273;
s = [1000 800 600 400 200];
ki = .00318;
Irr = 0.0622e-16;
k = 1.38 * 10(-23);
q = 1.602 * 10(-19);
FF = .74;Iscr = 8.21;Ar = 0.403750;A = 0.64616;Eg0 = 1.166;alpha = 0.473;beta = 636;
Eg = Eg0-(alpha*T*T)/(T+beta)*q;
Np = 4;
Ns = 60 ;
V0 =0:1:300;
for i = 1:5
Iph = (Iscr+ki*(T-Trefk))*((s(i))/1000);
Irs = Irr * ((T/Trefk)3) * exp(q * Eg/(k * A) * ((1/Trefk) - (1/T)));
I0 = Np * Iph - Np * Irs * (exp(q/(k * T * A) * V0./Ns) - 1);
P0 = V0.*I0;
N = (V0.*Iscr*FF)/(Ar*s(i));
figure(1)
plot(V0,I0);
axis([0 50 0 50]);
xlabel('voltage in volt');
ylabel('current in amp');
hold on;
figure(2)
plot(V0,P0);
axis([0 50 0 1500]);
xlabel('voltage in volts');
ylabel('power in watt');
hold on;
```

```
figure(3)
plot(I0,P0);
axis([0 40 0 1500]);
xlabel('current in amp');
ylabel('power in watt');
end
```

A2:for simulation of PV with varying temperature

```
T = [293 303 313 333 338];
Tref = 25;
Trefk = Tref+273;
s = 1000;
ki = 0.00023;
Iscr = 3.75;
Irr = 0.000021;
k = 1.38 * 10(-23);
q = 1.602 * 10(-19);
A = 2.15;
alpha = 0.473;
beta = 636;
Eg0 = 1.166;
for j=1:5
Eg = Eg0-(alpha*T(j)*T(j))/(T(j)+beta)*q;
end
Np = 54;
Ns = 2;
V0 = 0:1:300;
for i =1:5
Iph = (Iscr+ki*(T(i)-Trefk))*(s/100);
Irs = Irr * ((T(i)/Trefk)3) * exp(q * Eg/(k * A) * ((1/Trefk) - (1/T(i))));
I0 = Np * Iph - Np * Irs * (exp(q/(k * T(i) * A) * V0./Ns) - 1);
P0 = (V0.*I0);
figure(1)
plot(V0,I0);
axis([0 50 0 20]);
xlabel('voltage in volt');
ylabel('current in amp');
hold on;
figure(2)
plot(V0,P0);
axis([0 50 0 400]);
```

```
xlabel('voltage in volts');  
ylabel('power in watt');  
hold on;  
end
```

Annex A:Data sheet of solar panel



MODEL
KC200GT

THE NEW VALUE FRONTIER



KC200GT

HIGH EFFICIENCY MULTICRYSTAL PHOTOVOLTAIC MODULE



LISTED

HIGHLIGHTS OF KYOCERA PHOTOVOLTAIC MODULES

Kyocera's advanced cell processing technology and automated production facilities produce a highly efficient multicrystal photovoltaic module.

The conversion efficiency of the Kyocera solar cell is over 16%.

These cells are encapsulated between a tempered glass cover

and a pottant with back sheet to provide efficient protection from the severest environmental conditions.

The entire laminate is installed in an anodized aluminum frame to provide structural strength and ease of installation.

Equipped with plug-in connectors.



APPLICATIONS

KC200GT is ideal for grid tie system applications.

- Residential roof top systems
- Large commercial grid tie systems
- Water Pumping systems
- High Voltage stand alone systems
- etc.

QUALIFICATIONS

- **MODULE** : UL1703 certified
- **FACTORY** : ISO9001 and ISO 14001

QUALITY ASSURANCE

Kyocera multicrystal photovoltaic modules have passed the following tests.

- Thermal cycling test
- Thermal shock test
- Thermal / Freezing and high humidity cycling test
- Electrical isolation test
- Hail impact test
- Mechanical, wind and twist loading test
- Salt mist test
- Light and water-exposure test
- Field exposure test

LIMITED WARRANTY

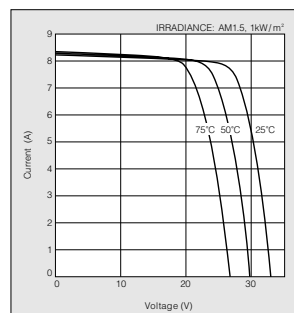
※ 1 year limited warranty on material and workmanship

※ 20 years limited warranty on power output: For detail, please refer to "category IV" in Warranty issued by Kyocera

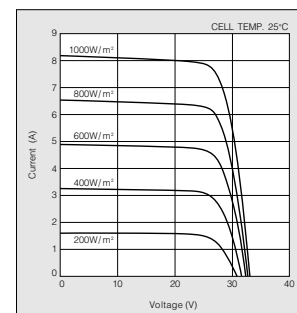
(Long term output warranty shall warrant if PV Module(s) exhibits power output of less than 90% of the original minimum rated power specified at the time of sale within 10 years and less than 80% within 20 years after the date of sale to the Customer. The power output values shall be those measured under Kyocera's standard measurement conditions. Regarding the warranty conditions in detail, please refer to Warranty issued by Kyocera)

ELECTRICAL CHARACTERISTICS

Current-Voltage characteristics of Photovoltaic Module KC200GT at various cell temperatures



Current-Voltage characteristics of Photovoltaic Module KC200GT at various irradiance levels

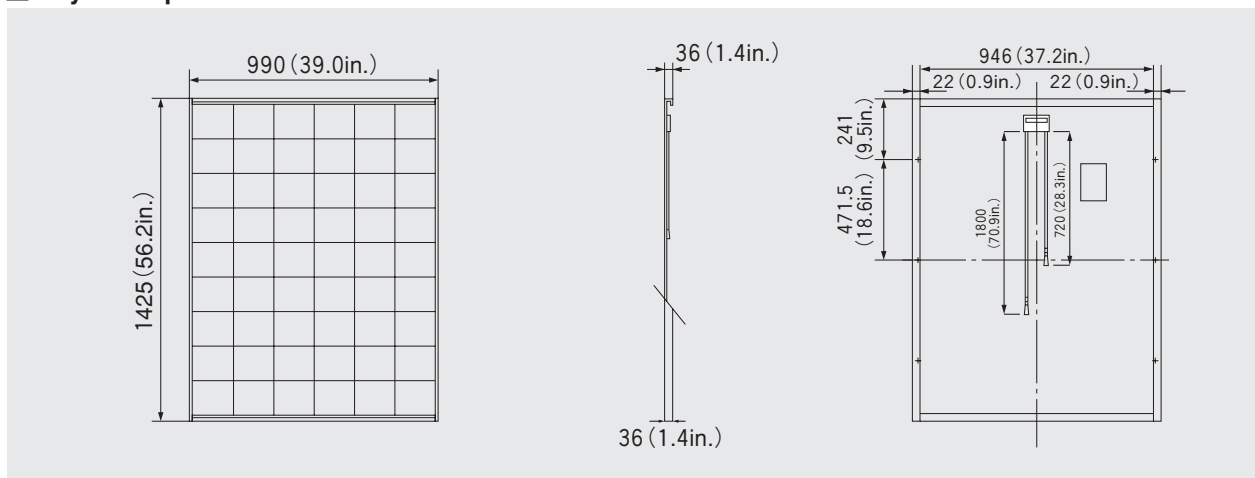


SPECIFICATIONS

KC200GT

Physical Specifications

Unit : mm (in.)



Specifications

Electrical Performance under Standard Test Conditions (*STC)	
Maximum Power (Pmax)	200W (+10%/−5%)
Maximum Power Voltage (Vmpp)	26.3V
Maximum Power Current (Impp)	7.61A
Open Circuit Voltage (Voc)	32.9V
Short Circuit Current (Isc)	8.21A
Max System Voltage	600V
Temperature Coefficient of Voc	−1.23×10 ⁻¹ V/°C
Temperature Coefficient of Isc	3.18×10 ⁻³ A/°C

*STC : Irradiance 1000W/m², AM1.5 spectrum, module temperature 25°C

Electrical Performance at 800W/m ² , NOCT, AM1.5	
Maximum Power (Pmax)	142W
Maximum Power Voltage (Vmpp)	23.2V
Maximum Power Current (Impp)	6.13A
Open Circuit Voltage (Voc)	29.9V
Short Circuit Current (Isc)	6.62A

NOCT (Nominal Operating Cell Temperature) : 47°C

Cells	
Number per Module	54

Module Characteristics	
Length × Width × Depth	1425mm(56.2in.)×990mm(39.0in.)×36mm(1.4in)
Weight	18.5kg(40.7lbs.)
Cable	(+)720mm(28.3in.), (-)1800mm(70.9in)

Junction Box Characteristics	
Length × Width × Depth	113.6mm(4.5in.)×76mm(3.0in.)×9mm(0.4in)
IP Code	IP65

Reduction of Efficiency under Low Irradiance	
Reduction	7.8%

Reduction of efficiency from an irradiance of 1000W/m² to 200W/m² (module temperature 25°C)

Please contact our office for further information



KYOCERA Corporation

KYOCERA Corporation Headquarters

CORPORATE SOLAR ENERGY DIVISION
6 Takeda Tobadono-cho
Fushimi-ku, Kyoto
612-8501, Japan
TEL:(81)75-604-3476 FAX:(81)75-604-3475
http://www.kyocera.com

KYOCERA Solar, Inc.

7812 East Acoma Drive
Scottsdale, AZ 85260, USA
TEL:(1)480-948-8003 or (800)223-9580 FAX:(1)480-483-6431
http://www.kyocerasolar.com

KYOCERA Solar do Brasil Ltda.

Av. Guignard 661, Loja A
22790-200, Recreio dos Bandeirantes, Rio de Janeiro, Brazil
TEL:(55)21-2437-8525 FAX:(55)21-2437-2338
http://www.kyocerasolar.com.br

KYOCERA Solar Pty Ltd.

Level 3, 6-10 Talavera Road, North Ryde
N.S.W. 2113, Australia
TEL:(61)2-9870-3948 FAX:(61)2-9888-9588
http://www.kyocerasolar.com.au/

KYOCERA Fin ceramics GmbH

Fritz Muller strasse 107, D-73730 Esslingen, Germany
TEL:(49)711-93934-917 FAX:(49)711-93934-950
http://www.kyocerasolar.de/

KYOCERA Asia Pacific Pte. Ltd.

298 Tiong Bahru Road, #13-03/05
Central Plaza, Singapore 168730
TEL:(65)6271-0500 FAX:(65)6271-0600

KYOCERA Asia Pacific Ltd.

Room 801-802, Tower 1 South Seas Centre, 75 Mody Road,
Tsimshatsui East, Kowloon, Hong Kong
TEL:(852)2-7237183 FAX:(852)2-7244501

KYOCERA Asia Pacific Ltd. Taipei Office

10 Fl., No.66, Nanking West Road, Taipei, Taiwan
TEL:(886)2-2555-3609 FAX:(886)2-2559-4131

KYOCERA(Tianjin) Sales & Trading Corporation

19F, Tower C HeQiao Building 8A GuangHua Rd.,
Chao Yang District, Beijing 100026, China
TEL:(86)10-6583-2270 FAX:(86)10-6583-2250

Annex B:Data sheet of Battery

6FM200S12(12V200Ah)

The AILE sealed lead-acid rechargeable battery (SLA battery) is leak-proof and maintenance free. The Superiority of SLA battery is derived from its uniquely efficient oxygen recombination technology. The oxygen evolved from the positive plates diffuses through the micro porous glass fiber mat to the negative plates where it is changed back to water by recombination reaction, eliminating the need for water addition .The result is a maintenance free battery.



Battery Construction

Component	Positive plate	Negative plate	Container	Cover	Safety valve	Terminal	Separator	Electrolyte
Raw material	Lead dioxide	Lead	ABS	ABS	Rubber	Copper	Fiberglass	Sulfuric acid

General Features

- Absorbent Glass Mat (AGM) technology for efficient gas recombination of up to 99% and freedom from electrolyte maintenance or water adding.
- Not restricted for air transport-complies with
- Can be mounted in any orientation.
- Computer designed lead, calcium tin alloy grid for high power density.
- Long service life, float or cyclic applications.
- Maintenance-free operation.
- Low self discharge.

Application

- Alarm System
- Medical Equipment
- Cable Television
- Control Equipment
- UPS
- Communication Equipment
- Toys
- Emergency power System
- Power Tools
- Security System

Specifications

Nominal voltage		12V	Capacity affected by temperature(20hr)	40°C	102%
Capacity(10hr, 25°C)		200Ah		25°C	100%
Design Life		10 Years		0°C	85%
				-15°C	65%
Dimension	Length	522mm(20.55inch)	Self-discharge (25 °C)	3 month	Remaining capacity: 91%
	Width	238mm(9.37inch)		6 month	Remaining capacity: 82%
	Height	218mm(8.58inch)		12 month	Remaining capacity: 65%
	Total height	238mm(9.37inch)			
Approx .weight		64kg(141.3lbs)	Normal operating temperature		25 °C + 3°C(77 F + 5F)
Capacity F (25 °C)	10hr rate	200Ah	Operating temperature range		-15 °C ~50°C (5~122F)
	3hr rate	160Ah	Float charging voltage(25°C)		13.60 to 13.80 V
	1hr rate	130Ah	Cyclic charging voltage(25 °C)		14.50 to 14.90 V
Internal Resistance(Full charged Battery 77 F (25 °C))		3mO	Maximum charging current		60A
			Terminal material		Copper
			Maximum Discharge current		1600A(5 sec)